Task 1 - Material Testing of Bionax Pipe and Joints

Submitted to:

Jeff Phillips
Western Regional Engineer
IPEX Management, Inc.
20460 Duncan Way
Langley, BC, Canada V3A 7A3
Ph: 604-534-8631
Fax: 604-534-7616
e-mail: Jeff.Phillips@ipexna.com

Submitted by:

School of Civil and Environmental Engineering
Cornell University
Hollister Hall
Ithaca, NY 14853

October, 2013

TABLE OF CONTENTS

LIST OF FIGURES

LIST OF FIGURES (continued)

LIST OF FIGURES (completed)

LIST OF TABLES

1. Introduction

This report is the first in a series of three reports to IPEX Management, Inc. and describes the results of Task 1 - Material Testing of Bionax Pipe and Joints. The work reported here is the result of a suite of tests to characterize the behavior of Bionax pipe and joints. Tests included basic material testing, and unpressurized and pressurized joint testing. All testing was performed in the Cornell University Large Scale Lifelines Testing Facility. IPEX provided all pipe materials and connection fittings. The primary pipe tested was Bionax 6"/150mm CIOD. Four of the tensile coupons were machined from Bionax 8″/200mm CIOD. The joint restraints, model UFR1559-C-6-I restraints for C909 PVCO, were manufactured by the Ford Meter Box Co., Inc.

This report presents the results of 1) tensile coupon tests on Bionax pipe to evaluate basic uniaxial stress-strain-strength response, 2) joint axial compression tests, and 3) joint axial tension tests. In the figures different symbols are used to differentiate data acquired with strain gages and the laser extensometer.

2. Tensile Coupon Testing

Coupon tests were performed on samples of the Bionax pipe to determine basic material properties. Several tensile coupon samples of pipe were cut in small “dogbones.” Table 2.1 lists the tests performed and the means of measurement for each test specimen. Seven specimens (T1, T2, T3, T4, T9, T10, and T11) were machined from 6-in. (150-mm)-diameter pipe sections. Four specimens (T5, T6, T7, and T8) were machined from 8-in. (200-mm)-diameter pipe sections. Figure 2.1 shows a schematic of the coupon geometry. Several specimens were instrumented with strain gage coupons to measure both axial and lateral strains, and all were instrumented with retro-reflective tape strips that are used with a laser extensometer. The strain gages represent “point” measurements of strain, using standard instrumentation methods. The laser extensometer measured the distance between edges on the reflective tape. Knowing the initial tape spacing, these measurements were used to calculate average strain over larger gage lengths.

Figure 2.2 is a photograph of a Bionax specimen in the testing apparatus. The photograph shows axial and horizontal gages on the test specimen. Also shown is the laser extensometer used to measure strains larger than those of the bondable strain gages.

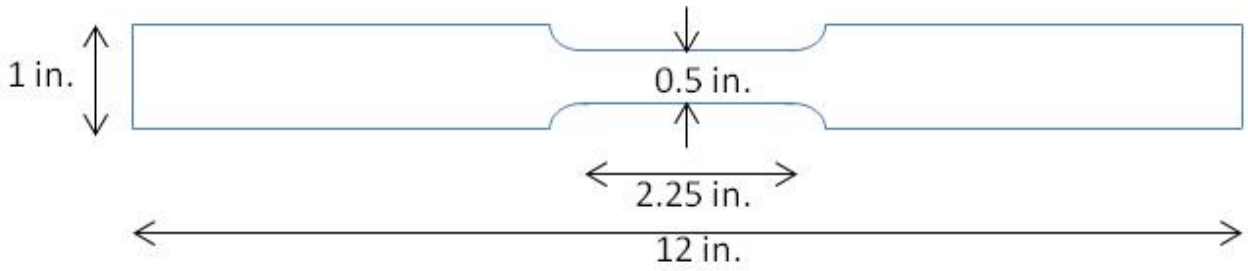

Figure 2.1. Schematic of the Bionax Tensile Coupon Specimen

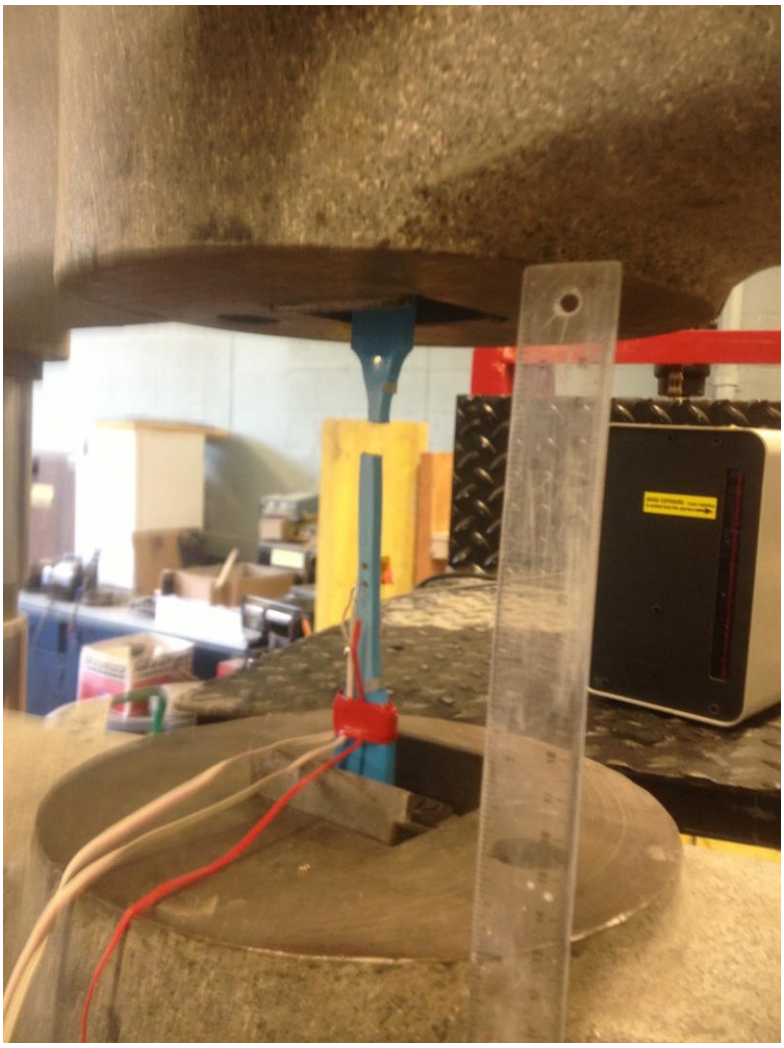

Figure 2.2. Bionax Tensile Test Coupon

Table 2.1. Bionax Tensile Test Specimen Information

Specimen	Test Displacement Rate		Instrumentation		
	(in./min)	(%/min.)	Strain Gage - Axial	Strain Gage - Horizontal	Laser Extensometer - Axial
T1	0.49	24	x	x	x
T2	0.36	18			x
T3	0.46	23	x		x
T4	0.46	23	x		x
T5	0.88	44		x	x
T6	0.76	38			x
T7	0.43	22	x		x
T8	1.43	72			x
T9	1.86	93			x
T10	1.84	92			x
T11	3.12	156			x

Figure 2.3 shows the axial strains measured with strain gages at the “front” and “back” of coupon T1, and also includes extensometer data at the “front” of the specimen. The “front” side refers to the coupon surface that coincides with the outer surface of the Bionax Pipe, while the “back” refers to the inner surface of the pipe. Note that nominal strains are conventional engineering strains of $\varepsilon_{nom} = \Delta L/L$ where ΔL is the change in length and L is the original length. Also, nominal stress is $\sigma_{nom} = P/A$ where P is the axial force and A is the original specimen cross sectional area, A, uncorrected for axial strain. Figure 2.4 shows the axial strains for specimen T1 at larger strains. The peak stress for specimen T1 was 8.01 ksi (55.2 MPa) at an axial strain of 0.0515.

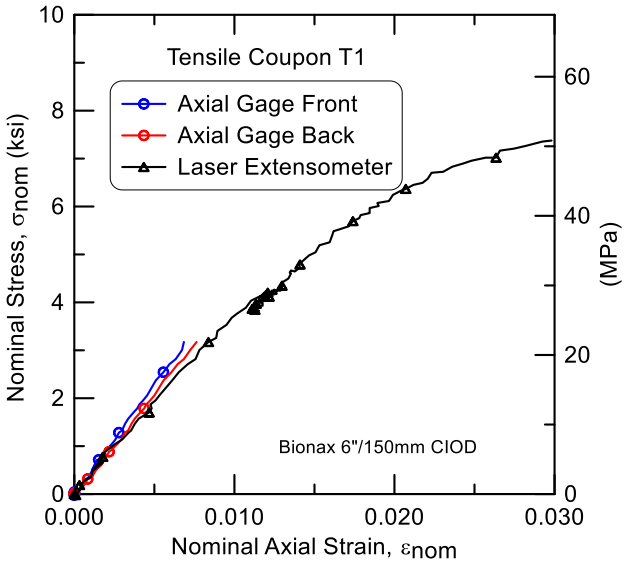

Figure 2.3. Coupon T1 Bionax Axial Stress-Stain at Small Strains

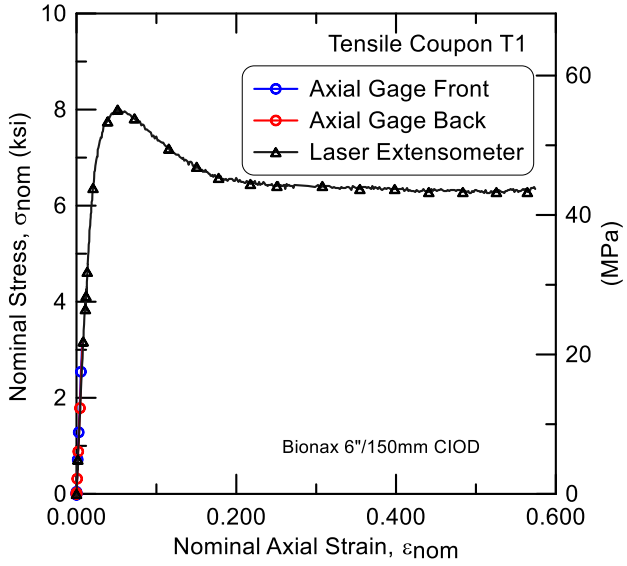

Figure 2.4. Coupon T1 Bionax Axial Stress-Stain at Large Strains

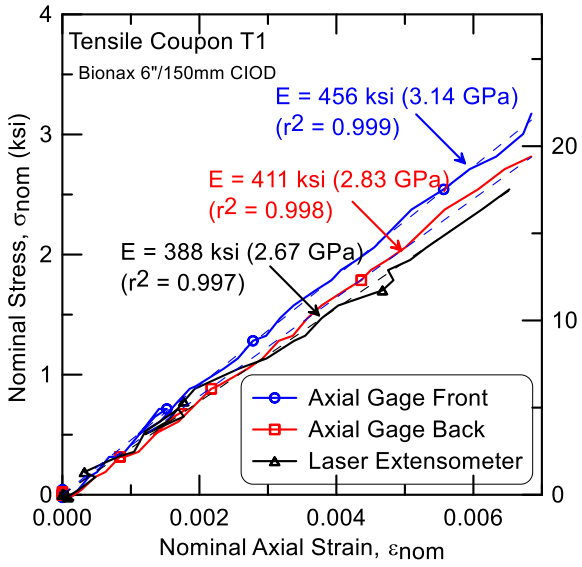

Figure 2.5. Coupon T1 Bionax Young's Moduli at Axial Strains Less than 0.007

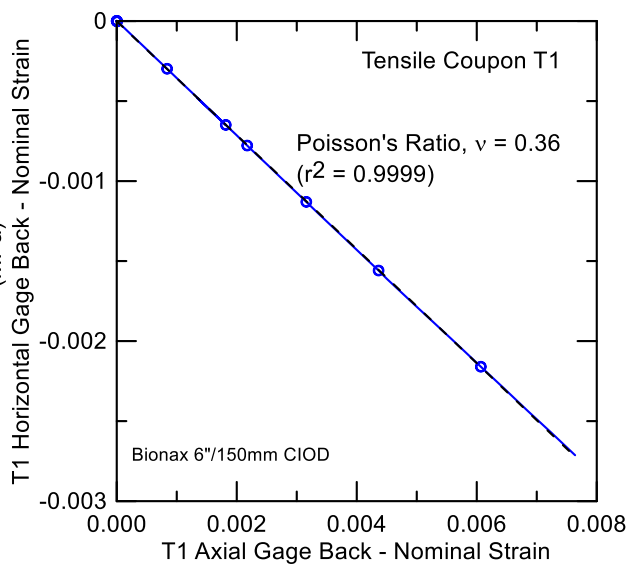

Figure 2.6 Coupon T1 Bionax Horizontal vs. Axial Strains

Young's modulus, E, from specimen T1 is determined at axial strains less than 0.007, where the stress-strain curve is approximately linear. Young's modulus, E, is the ratio of nominal axial stress to nominal axial strain for uniaxial loading. The stress levels from the three gages also are roughly 3 ksi (20.7 MPa) at this strain level. Figure 2.5 shows the regression curves (fitted through the origin) for the three axial instruments in coupon T1 at strains less than 0.007. Young's modulus from the front gage data is E = 456 ksi (3.14 GPa) from the back gage data is E = 411 ksi (2.83 GPa) and from the extensometer data is E = 388 ksi (2.67 GPa). Figure 2.6 shows axial and horizontal strains for specimen T1. In the figure strains are plotted for only positive axial strains and negative horizontal strains. This is because the initial horizontal strains indicated seating irregularities at very small strains. The horizontal and axial strains can be used to determine Poisson's ratio, $\nu = -\varepsilon_h/\varepsilon_a$, where ε_h is the nominal horizontal strain and ε_a is the nominal axial strain for the condition of uniaxial loading. The test data from coupon T1 indicate that Poisson's ratio for the Bionax specimen is $\nu = 0.36$.

Figure 2.7 shows the axial strains measured for coupon T2 with the extensometer at relatively small nominal strains. Figure 2.8 shows the axial strains for specimen T2 at larger strains. The peak stress for specimen T2 was 7.91 ksi (54.5 MPa) at an axial strain of 0.0548. Figure 2.9 shows the regression curve (fitted through the origin) for the extensometer data for coupon T2 at strains less than 0.007. Young's modulus from the extensometer data is E = 418 ksi (2.88 GPa).

Figure 2.10 shows the axial strains measured for coupon T3 with the "front" axial gage and the extensometer at relatively small nominal strains. In the figure the dashed line labeled "Offset Correction" on the extensometer data is due to apparent strains caused by seating adjustments in the mechanical testing apparatus. The dashed line on Figure 2.10 shows the extensometer data corrected for this apparent offset. Figure 2.11 shows the extensometer axial strains for specimen T3 at larger strains. The peak stress for specimen T3 was 7.64 ksi (52.6 MPa) at an axial strain of 0.0532. Figure 2.12 shows the regression curve (fitted through the origin) for the axial strain gage and extensometer data for coupon T3 at strains less than 0.007. Young's modulus from the strain gage data is E = 466 ksi (3.21 GPa) and that from the extensometer data is E = 307 ksi (2.11 GPa). Young's modulus from the extensometer data appears to be unusually low.

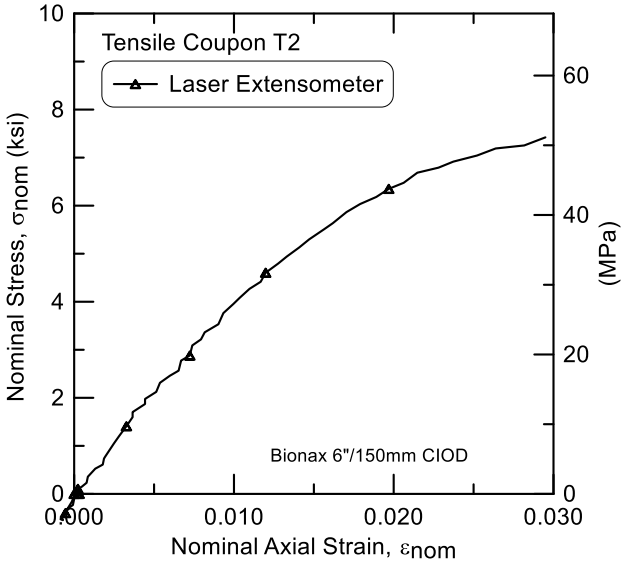

Figure 2.7. Coupon T2 Bionax Axial Stress-Strain at Small Strains

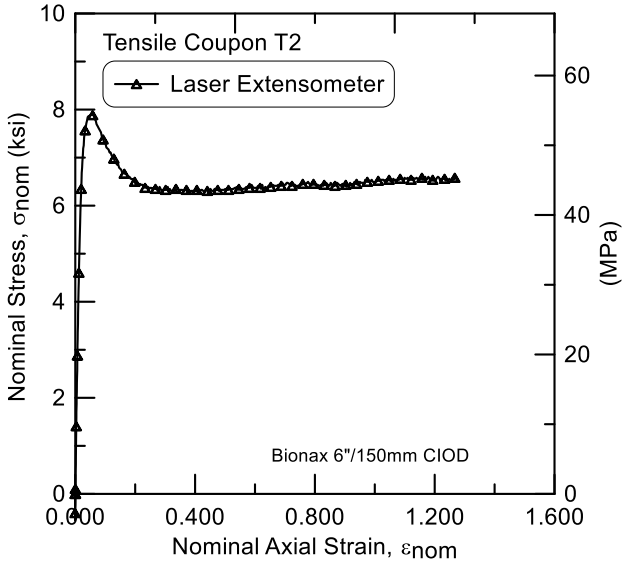

Figure 2.8. Coupon T2 Bionax Axial Stress-Strain at Large Strains

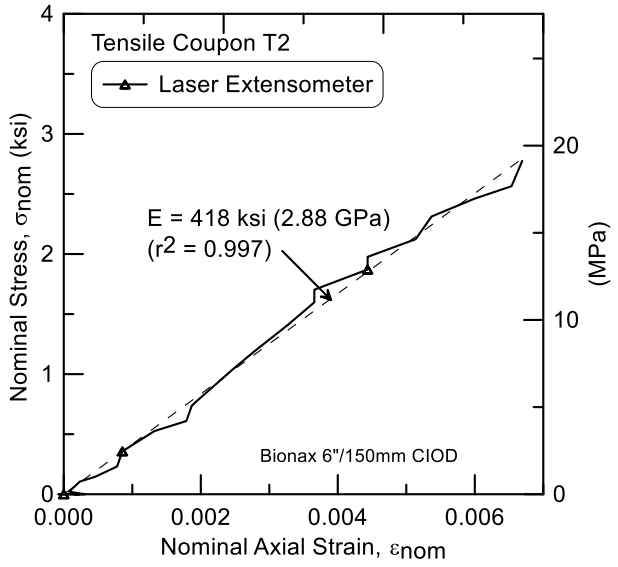

Figure 2.9. Coupon T2 Bionax Young's Modulus at Axial Strains Less than 0.007

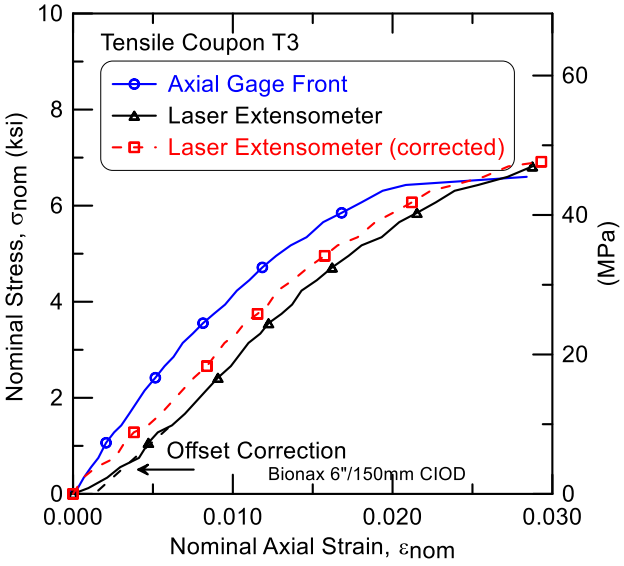

Figure 2.10. Coupon T3 Bionax Axial Stress-Strain at Small Strains

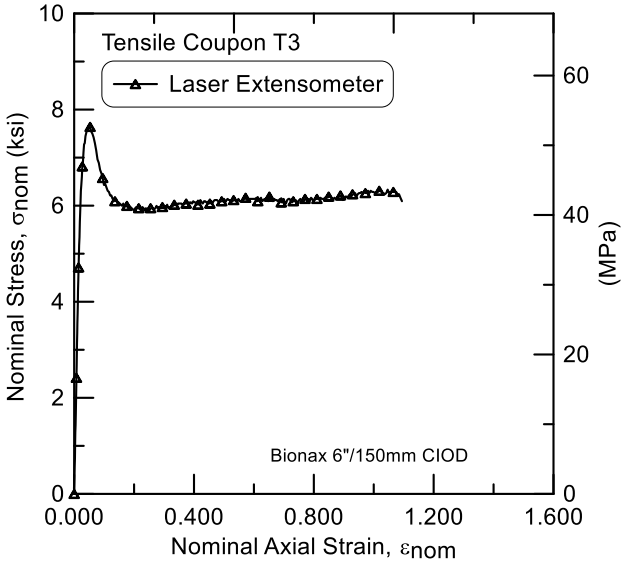

Figure 2.11. Coupon T3 Bionax Axial Stress-Strain at Large Strains

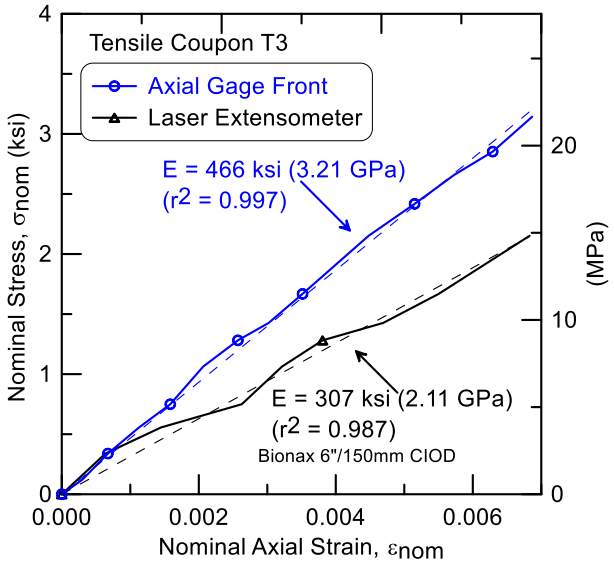

Figure 2.12. Coupon T3 Bionax Young's Moduli at Axial Strains Less than 0.007

Figure 2.13 shows the axial strains measured for coupon T4 with the "front" axial gage and the extensometer at relatively small nominal strains. Figure 2.14 shows the extensometer axial strains for specimen T4 at larger strains. The peak stress for specimen T4 was 8.14 ksi (56.1 MPa) at an axial strain of 0.0486. Figure 2.15 shows the regression curve (fitted through the origin) for the axial strain gage and extensometer data for coupon T4 at strains less than 0.007. Young's modulus from the strain gage data is E = 492 ksi (3.39 GPa) and that from the extensometer data is E = 423 ksi (2.91 GPa).

Figure 2.16 shows the axial strains measured for coupon T5 the extensometer at relatively small nominal strains. T5 was cut from Bionax 8″/200. Figure 2.17 shows the extensometer axial strains for specimen T5 at larger strains. The peak stress for specimen T5 was 8.35 ksi (57.5 MPa) at an axial strain of 0.0500. Figure 2.18 shows the regression curve (*not* fitted through the origin) for the extensometer data for coupon T5 at strains less than 0.007. Young's modulus from the extensometer data is E = 465 ksi (3.20 GPa). Figure 2.19 shows horizontal strains from the strain gage vs. the laser extensometer axial strains for specimen T5. In the figure strains are plotted for only positive axial strains and negative horizontal strains, and for axial strains less than 0.08. At larger axial strains the gage data become very nonlinear. The test data from coupon T5 indicate that Poisson's ratio for the Bionax specimen is $\nu = 0.36$.

Figure 2.20 shows the axial strains measured for coupon T6 extensometer strains at relatively small nominal strains. T6 was cut from Bionax 8″/200mm. Figure 2.21 shows the axial strains for specimen T6 at larger strains. The peak stress for specimen T6 was 8.58 ksi (59.1 MPa) at an axial strain of 0.0479. Figure 2.22 shows the regression curve (fitted through the origin) for the extensometer data for coupon T6 at strains less than 0.007. Young's modulus from the extensometer data is E = 468 ksi (3.22 GPa).

Figure 2.23 shows the axial strains measured for coupon T7 with the "front" axial gage and the extensometer at relatively small nominal strains. T7 was cut from Bionax 8″/200mm. Figure 2.24 shows the axial strains for specimen T7 at larger strains. The peak stress for specimen T7 was 8.20 ksi (56.5 MPa) at an axial strain of 0.0549. Figure 2.25 shows the regression curve (fitted through the origin) for the axial strain gage and extensometer data for coupon T7 at strains less than 0.007. Young's modulus from the strain gage data is E = 583 ksi (4.02 GPa) and that from the

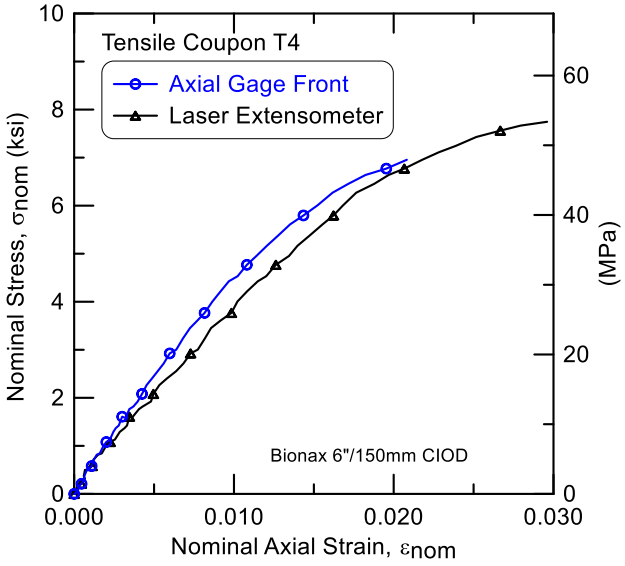

Figure 2.13. Coupon T4 Bionax Axial Stress-Strain at Small Strains

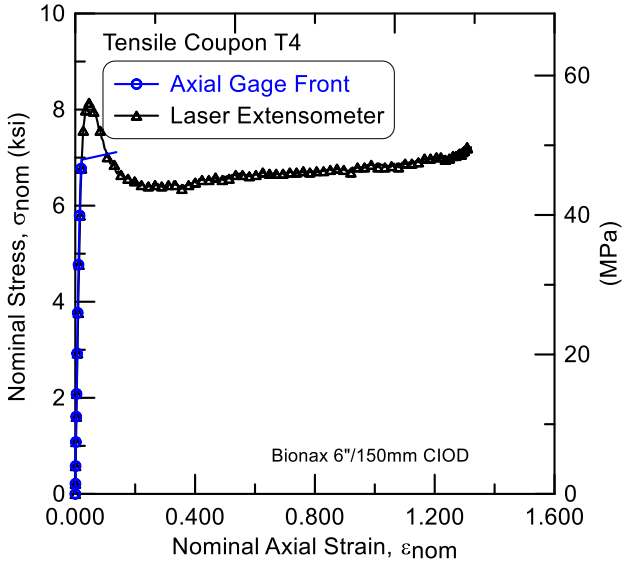

Figure 2.14. Coupon T4 Bionax Axial Stress-Strain at Large Strains

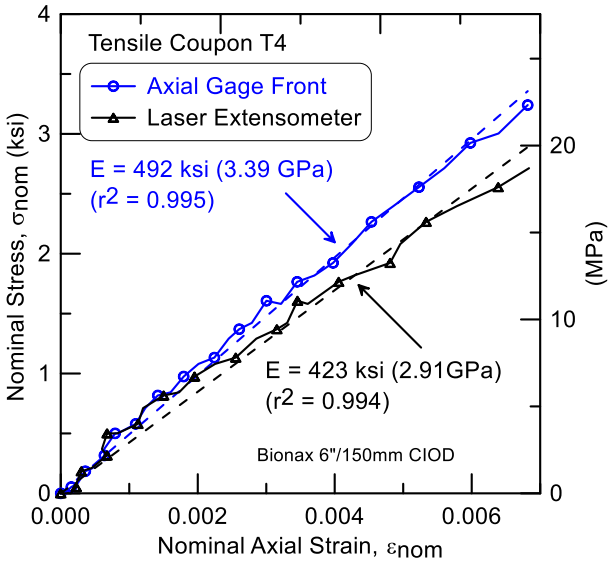

Figure 2.15. Coupon T4 Bionax Young's Moduli at Axial Strains Less than 0.007

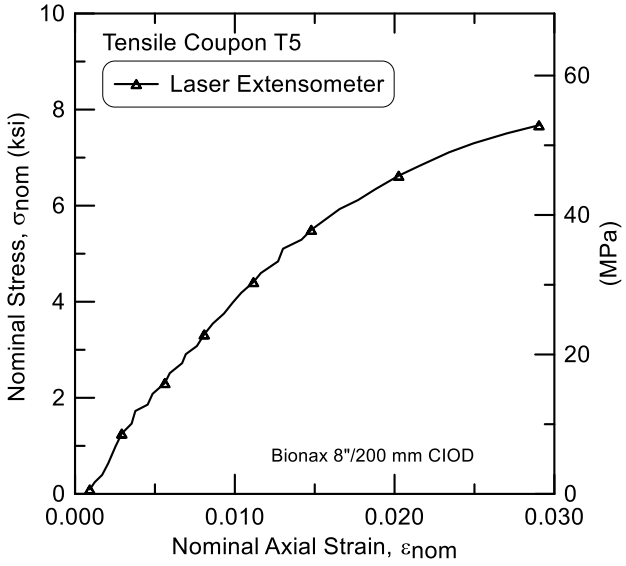

Figure 2.16. Coupon T5 Bionax Axial Stress-Strain at Small Strains

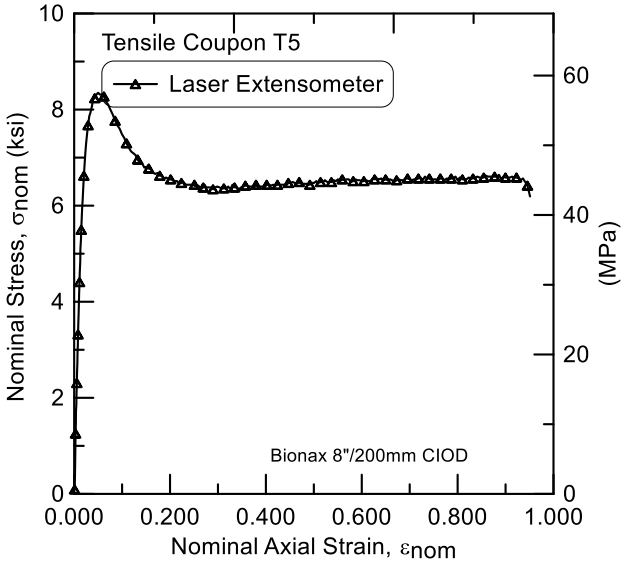

Figure 2.17. Coupon T5 Bionax Axial Stress-Strain at Large Strains

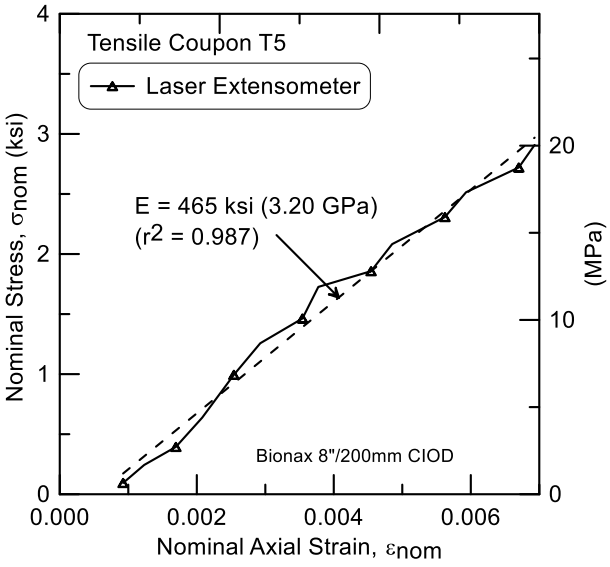

Figure 2.18. Coupon T6 Bionax Young's Modulus at Axial Strains Less than 0.007

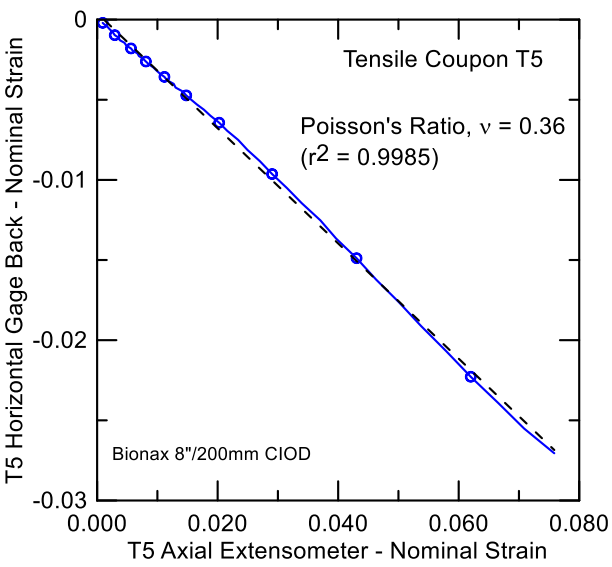

Figure 2.19. Coupon T5 Bionax Horizontal vs. Axial Strains

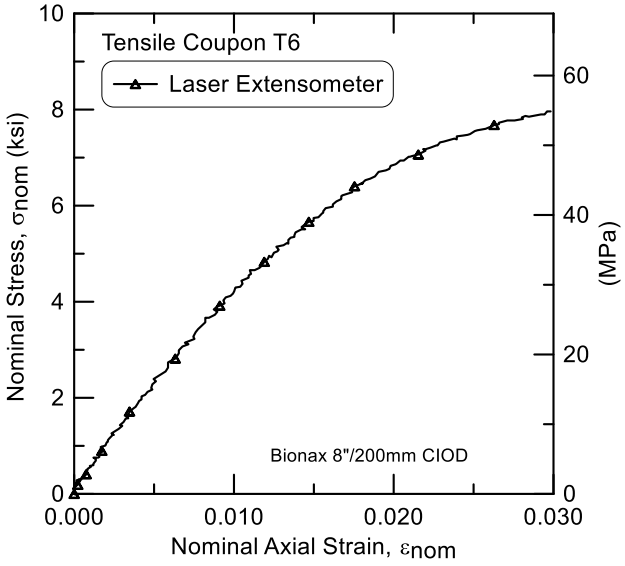

Figure 2.20. Coupon T6 Bionax Axial Stress-Strain at Small Strains

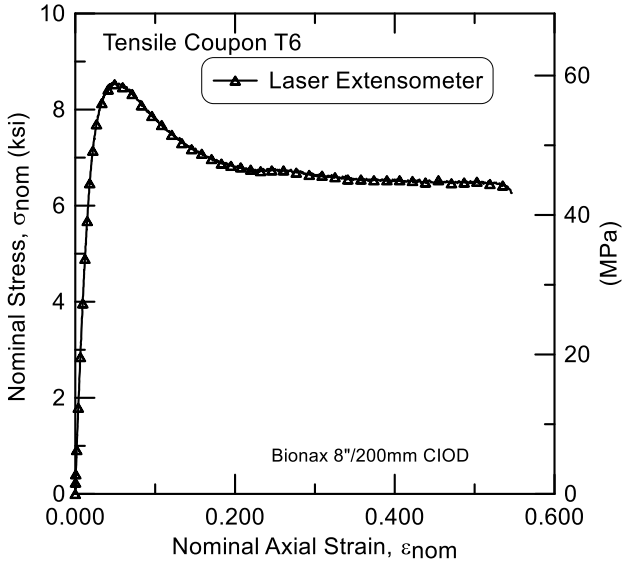

Figure 2.21. Coupon T6 Bionax Axial Stress-Strain at Large Strains

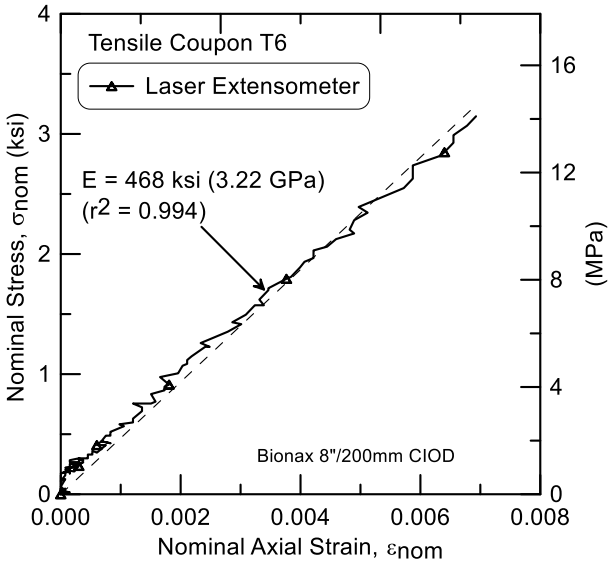

Figure 2.22. Coupon T6 Bionax Young's Modulus at Axial Strains Less than 0.007

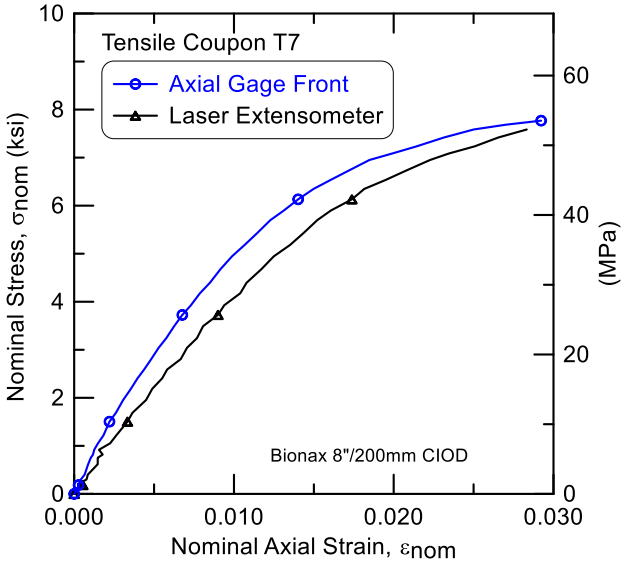

Figure 2.23. Coupon T7 Bionax Axial Stress-Strain at Small Strains

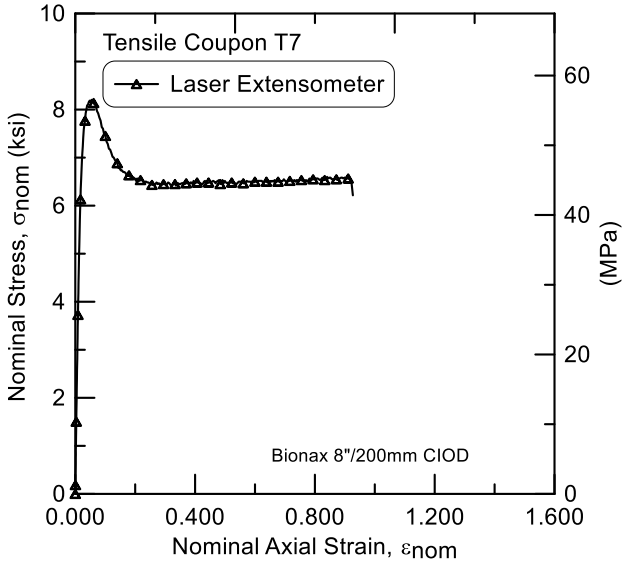

Figure 2.24. Coupon T7 Bionax Axial Stress-Strain at Large Strains

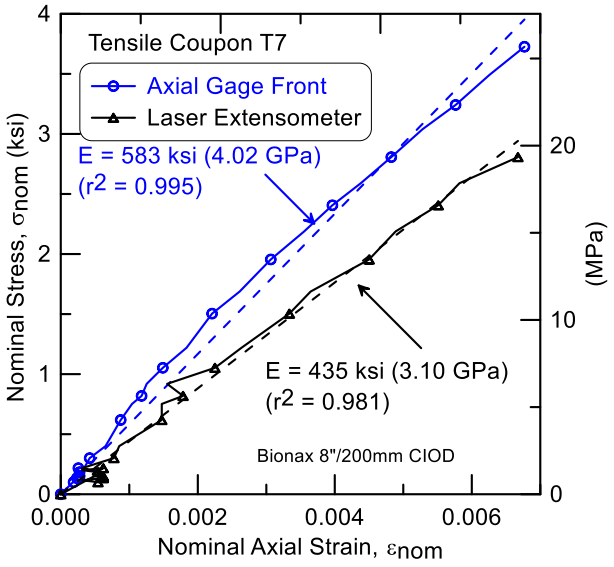

Figure 2.25. Coupon T7 Bionax Young's Moduli at Axial Strains Less than 0.007

extensometer data is E = 435 ksi (3.00 GPa). For these data, the modulus calculated from the strain gage appears high.

Figure 2.26 shows the axial strains measured for coupon T8 with the extensometer data at relatively small nominal strains. T8 was cut from Bionax 8″/200mm. Figure 2.27 shows the axial strains for specimen T8 at larger strains. The peak stress for specimen T8 was 8.94 ksi (61.6 MPa) at an axial strain of 0.0522. Figure 2.28 shows the regression curve (fitted through the origin) for the axial strain gage and extensometer data for coupon T8 at strains less than 0.007. Young's modulus from extensometer data is E = 368 ksi (2.54 GPa).

Figure 2.29 shows the axial strains measured for coupon T9 with the strain gage data at relatively small nominal strains. Figure 2.30 shows the axial strains for specimen T9 at larger strains. The peak stress for specimen T9 was 8.75 ksi (60.3 MPa) at an axial strain of 0.0485. Figure 2.31 shows the regression curve (fitted through the origin) for the axial strain gage data for coupon T9 at strains less than 0.007. Young's modulus from strain gage data is E = 477 ksi (3.29 GPa).

Figure 2.32 shows the axial strains measured for coupon T10 with the strain gage data at relatively small nominal strains. Figure 2.33 shows the axial strains for specimen T10 at larger strains. The peak stress for specimen T10 was 8.46 ksi (58.3 MPa) at an axial strain of 0.0460. Figure 2.34 shows the regression curve (fitted through the origin) for the axial strain gage data for coupon T10 at strains less than 0.007. Young's modulus from strain gage data is E = 398 ksi (2.74 GPa).

Figure 2.35 shows the axial strains measured for coupon T11 with the strain gage data at relatively small nominal strains. Figure 2.36 shows the axial strains for specimen T11 at larger strains. The peak stress for specimen T11 was 8.80 ksi (60.6 MPa) at an axial strain of 0.0506. Figure 2.37 shows the regression curve (*not* fitted through the origin) for the axial strain gage data for coupon T11 at strains less than 0.007. Young's modulus from strain gage data is E = 433 ksi (2.99 GPa).

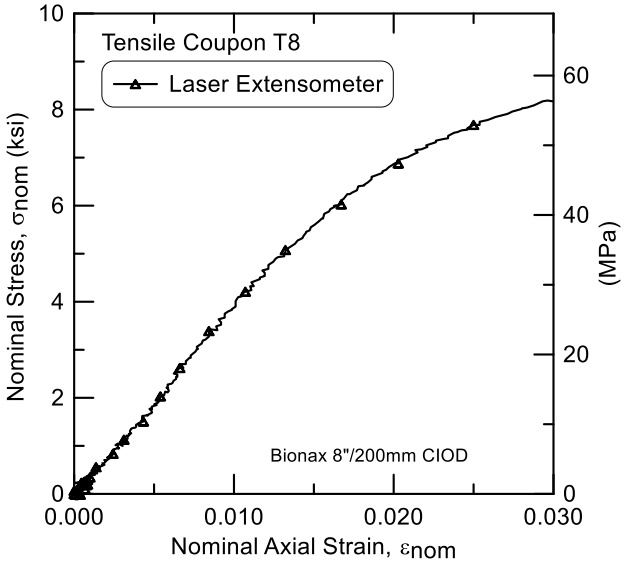

Figure 2.26. Coupon T8 Bionax Axial Stress-Strain at Small Strains

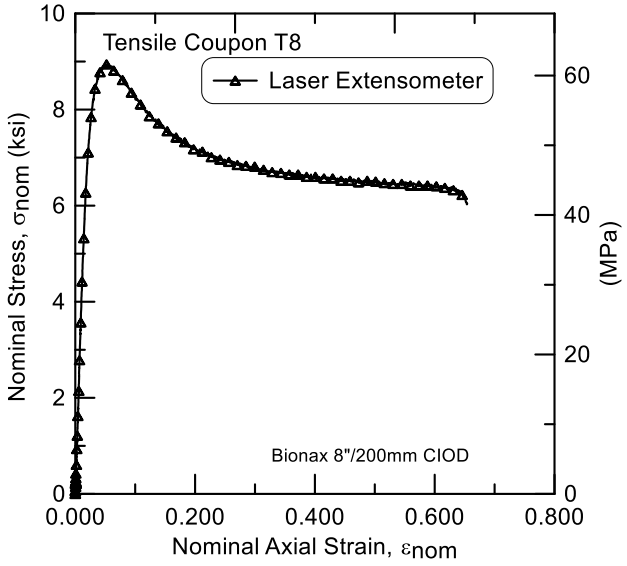

Figure 2.27. Coupon T8 Bionax Axial Stress-Strain at Large Strains

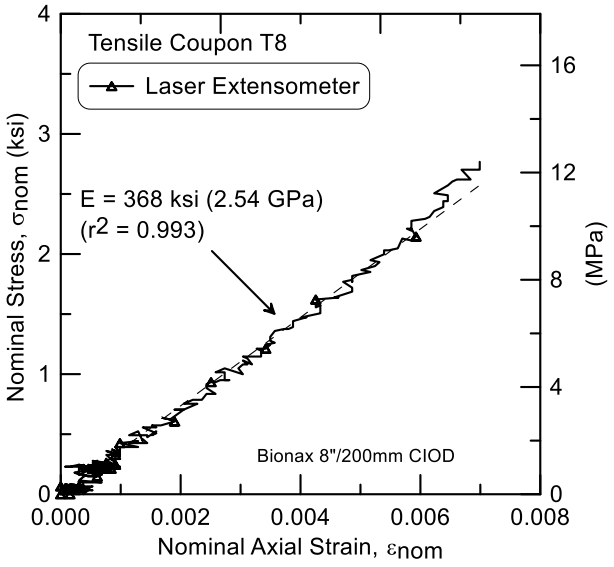

Figure 2.28. Coupon T8 Bionax Young's Modulus at Axial Strains Less than 0.007

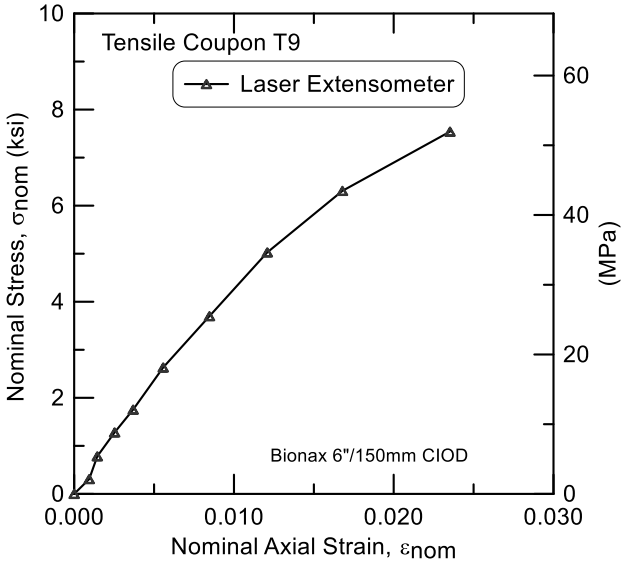

Figure 2.29. Coupon T9 Bionax Axial Stress-Strain at Small Strains

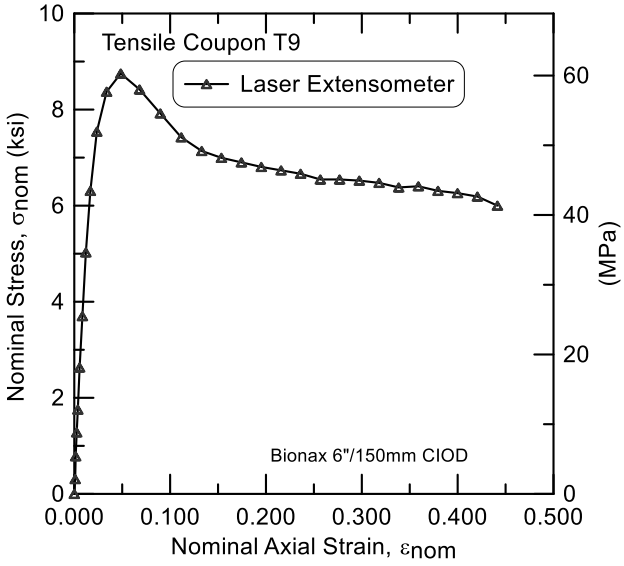

Figure 2.30. Coupon T9 Bionax Axial Stress-Strain at Large Strains

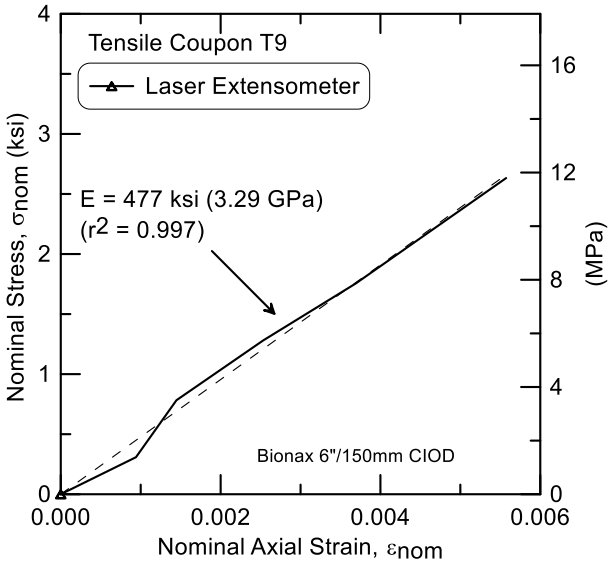

Figure 2.31. Coupon T9 Bionax Young's Modulus at Axial Strains Less than 0.007

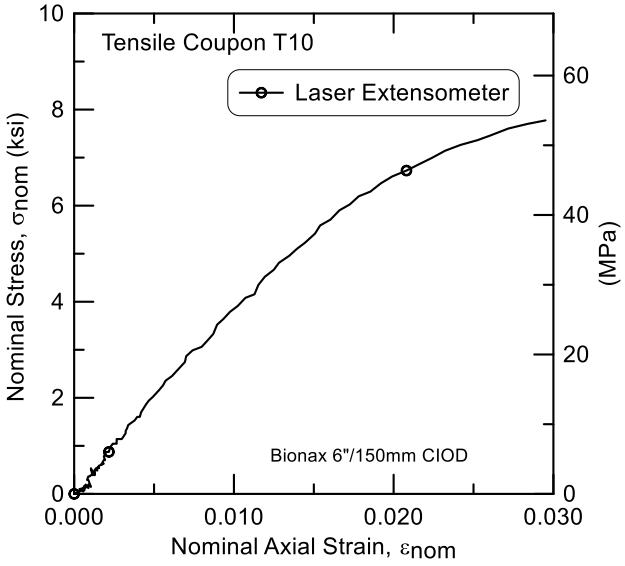

Figure 2.32. Coupon T10 Bionax Axial Stress-Stain at Small Strains

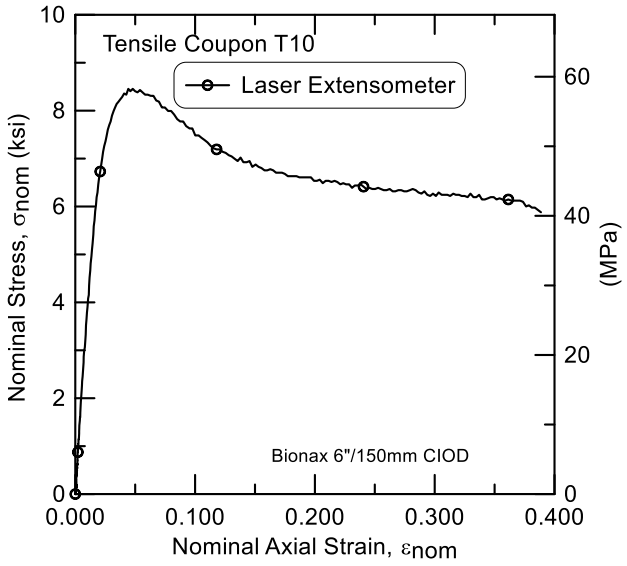

Figure 2.33. Coupon T10 Bionax Axial Stress-Stain at Large Strains

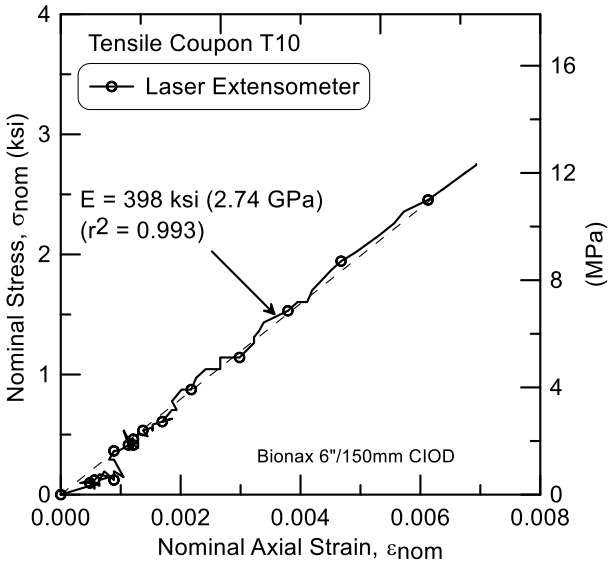

Figure 2.34. Coupon T10 Bionax Young's Modulus at Axial Strains Less than 0.007

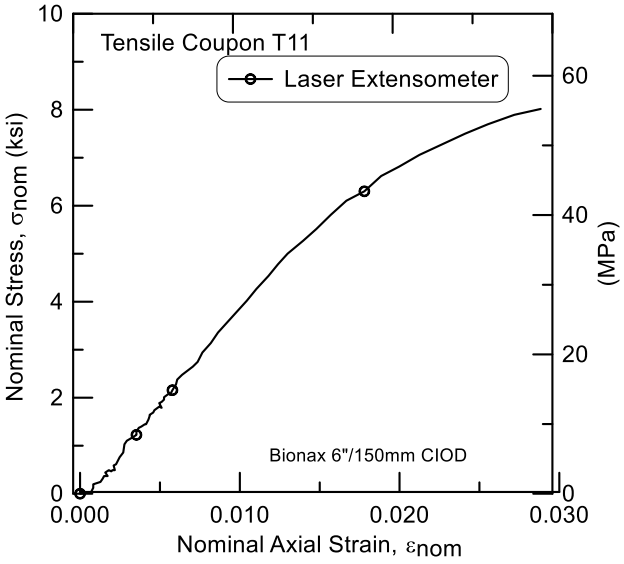

Figure 2.35. Coupon T11 Bionax Axial Stress-Stain at Small Strains

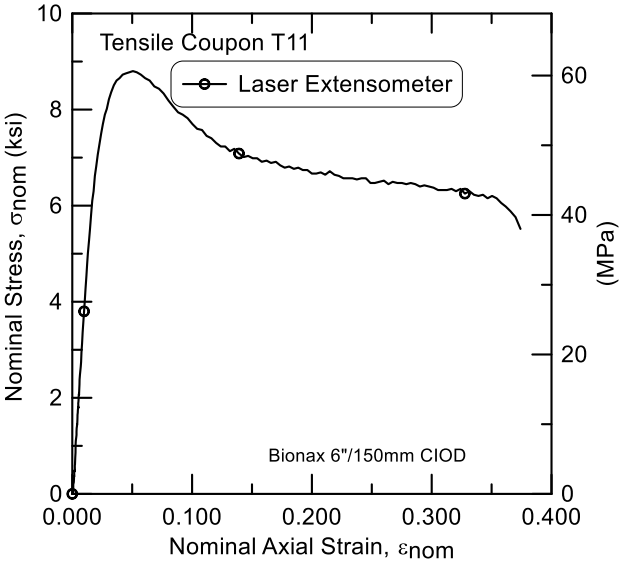

Figure 2.36. Coupon T11 Bionax Axial Stress-Stain at Large Strains

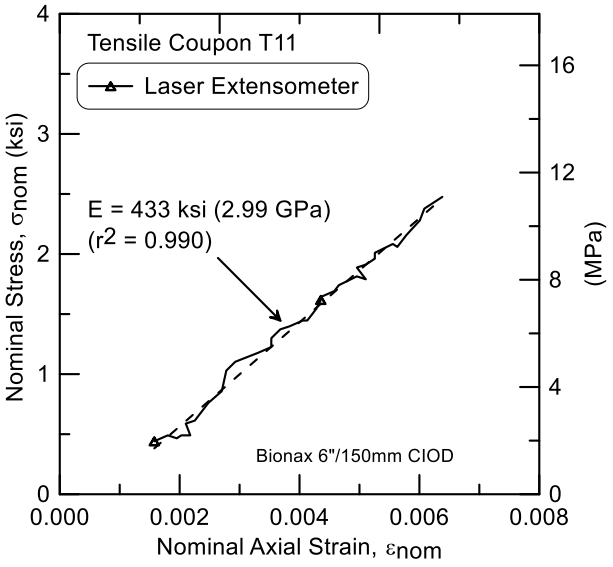

Figure 2.37. Coupon T11 Bionax Young's Modulus at Axial Strains Less than 0.007

The tensile coupons for the Bionax were taken from the 6-in. (150-mm) - diameter pipe and tested under similar conditions. All specimens were made from samples taken from the longitudinal direction of the pipe. Figures 2.38 and 2.39 show the stress-strain results (mostly extensometer data) from all eleven tests. Table 2.2 summarizes the test data, giving moduli, Poisson's ratio, maximum stress, and the strain at the maximum stress. The average Young's Modulus for strains less than 0.007 from the extensometer data is 416 ksi (2.89 GPa). The modulus determined from Specimen T3 is very low. The average Young's modulus from the strain gage data is roughly 16% higher at 481 ksi (3.32 GPa). Poisson's ratio measured in two tests was 0.36. The average maximum nominal maximum stress for all specimens is 8.34 ksi (57.5 MPa) corresponding to an average nominal axial strain of 0.0507.

Table 2.2. Bionax Tensile Test Summary

Specimen	Young's Modulus, E, at Strains Less than 0.007		Poisson's Ratio	Maximum Stress ksi (MPa)	Strain at Maximum Stress
	Laser Extensometer ksi (GPa)	Strain Gage ksi (GPa)			
T1	388 (2.67)	456 (3.14)	0.36	8.01 (55.2)	0.0515
T1		411 (2.83)			
T2	418 (2.88)			7.91 (54.5)	0.0548
T3	307 (2.12)	466 (3.21)		7.64 (52.6)	0.0532
T4	423 (2.91)	492 (3.39)		8.14 (56.1)	0.0486
T5	465 (3.20)		0.36	8.35 (57.5)	0.0500
T6	468 (3.22)			8.58 (59.1)	0.0479
T7	435 (3.00)	583 (4.02)		8.20 (56.5)	0.0549
T8	368 (2.54)			8.94 (61.6)	0.0522
T9	477 (3.29)			8.75 (60.3)	0.0485
T10	398 (2.74)			8.46 (58.3)	0.0460
T11	433 (2.98)			8.80 (60.6)	0.0506
Average	416 (2.87)	481 (3.32)	0.36	8.34 (57.5)	0.0507
Stdev	49.8 (0.34)	63.8 (0.44)	-	0.39 (2.7)	0.0028

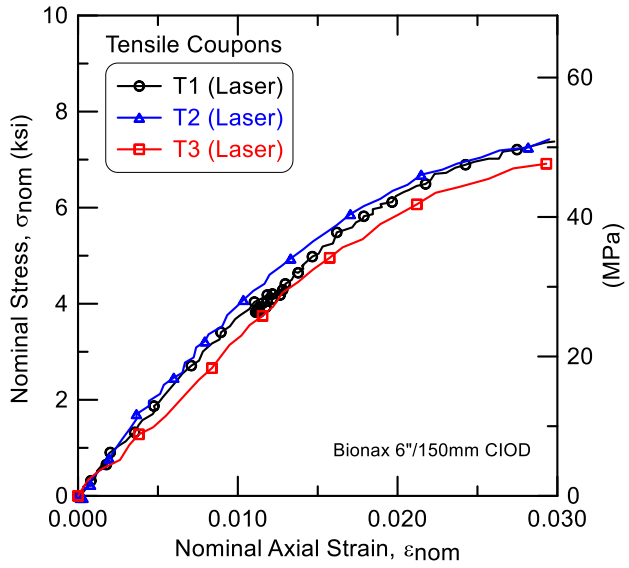

a) Coupons T1, T2, and T3

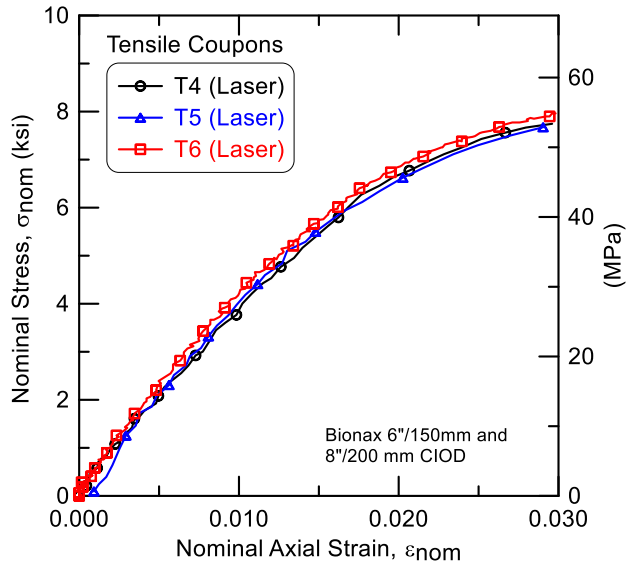

b) Coupons T4, T5, and T6

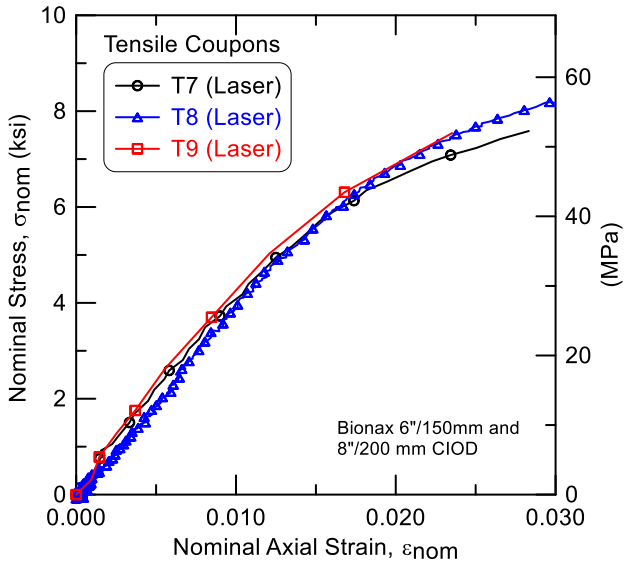

c) Coupons T7, T8, and T9

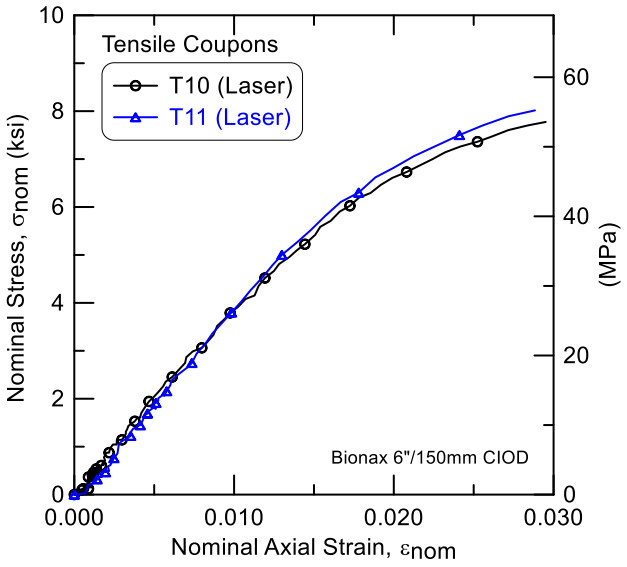

d) Coupons T10 and T11

Figure 2.38. All Bionax Coupon Stress – Strain at Relatively Small Strains

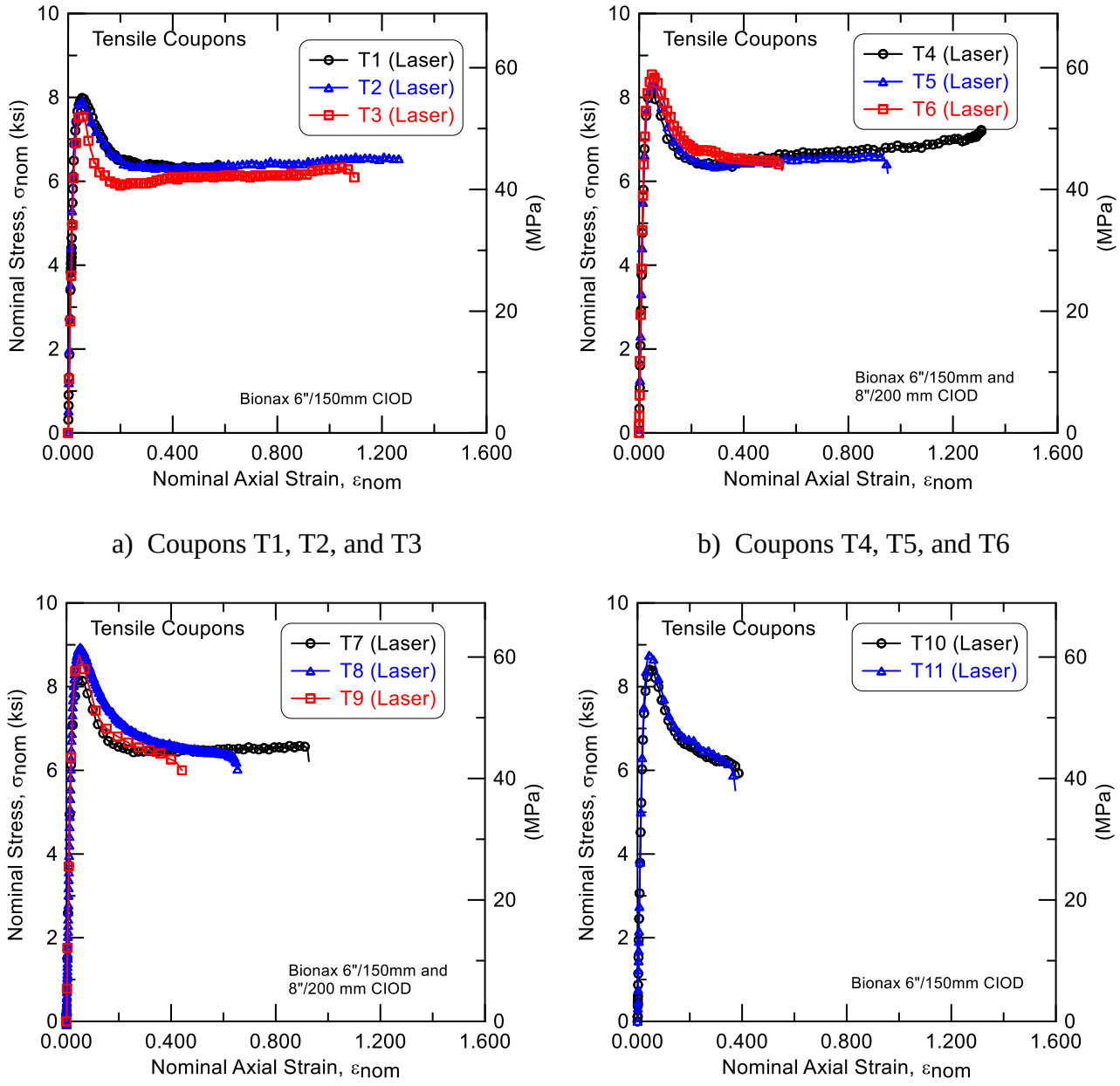

a) Coupons T1, T2, and T3

b) Coupons T4, T5, and T6

c) Coupons T7, T8, and T9

d) Coupons T10 and T11

Figure 2.39. All Bionax Coupon Stress - Strain at Relatively Large Strains

The moduli data were used in single factor Analysis of Variance (ANOVA) to evaluate if the mean value from the extensometer data and strain gage data could be considered the same. At the 95% confidence level the two data sets can be considered the same. The global average Young's modulus from the Bionax tensile coupons was E = 437 ksi (3.01GPa) with a standard deviation of 63.7 ksi (0.44 GPa).

Figure 2.40 shows the moduli at strains less than 0.007 with respect to strain rate. For the range of strain rates used there is no clear evidence for rate dependency. Also shown in the figure is a solid line showing the average value for all test specimens and dashed lines indicating the 95% confidence interval around mean value, which is +/– 29.7 ksi (0.21 GPa).

The average stress-strain curve for the Bionax was converted into true stress – true strain data as shown in Figure 2.41. The elastic stress vs. strain relationship is shown, with the plastic stress-strain curve. These relationships were used in nonlinear numerical modeling for Task 3, involving the large-scale split basin tests.

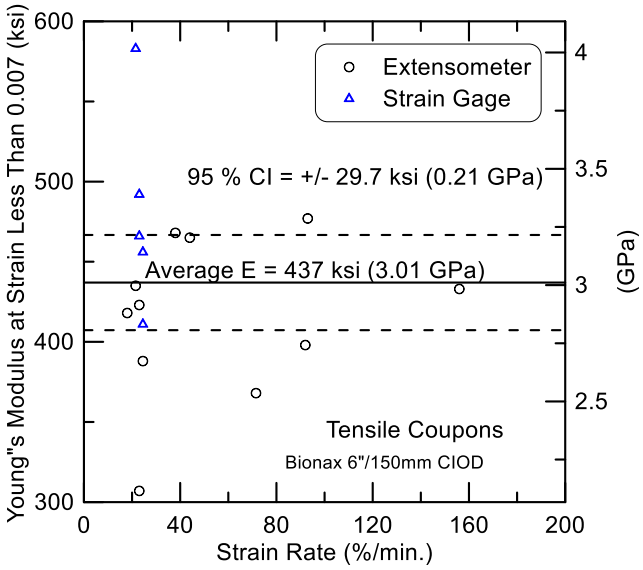

Figure 2.40. Average Bionax Young's Modulus

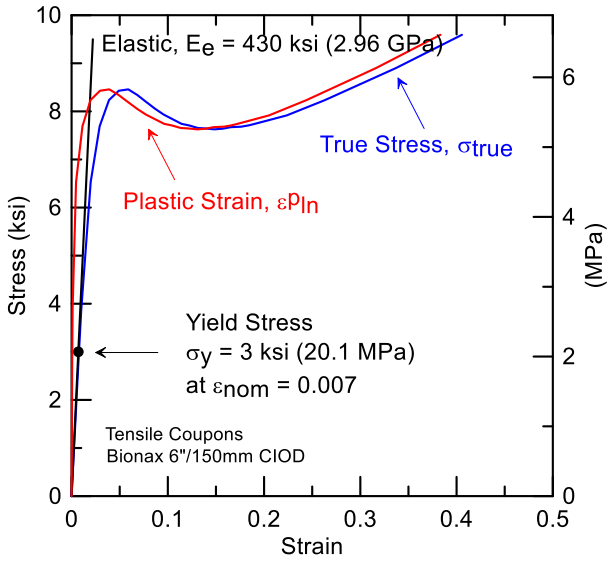

Figure 2.41. Bionax Elastic-Plastic Stress Strain Curves

3. Joint Compression Tests

Two compression tests were performed on nominal 6 in. (150 mm) Bionax piping. Two 57-in. (144.7-cm)-long sections were tested. The bell-and-spigot section was pressurized and tested in compression. Specimen C1 did not have a joint restraint. Specimen C2 had a UFR1559-C-6-I restraint. The pipes were fitted with end caps and pressurized with water to approximately 85 psi (586 kPa).

3.1 Without Joint Restraint

Figure 3.1 is a photo of the setup for test C1. In the photograph, north is to the right. String potentiometers were positioned at the crown, invert, east springline and west springline. Strain gages were mounted at the crown and invert roughly 18 in. (457 mm) north of the joint. The maximum compressive force applied in test C1 was -12.1 kips (-54.2 kN), when the test was stopped at a displacement of -5.7 in. (-144.8 mm). Figure 3.2 shows specimen C1 at the end of the test. The bulge on the bell side of the joint marks the location to which the spigot was pushed into the pipe on the left side of the joint. Figure 3.3 shows a view of the interior of the test C1 specimen where the spigot has been pushed into the bell side. The spigot has pushed smoothly into and through the bell, primarily by inducing an increase in bell end diameter.

The compressive forces vs. joint closings are shown in Figure 3.4. All of the string pot measurements were nearly identical. The strains at the crown and invert are shown in Figure 3.5.

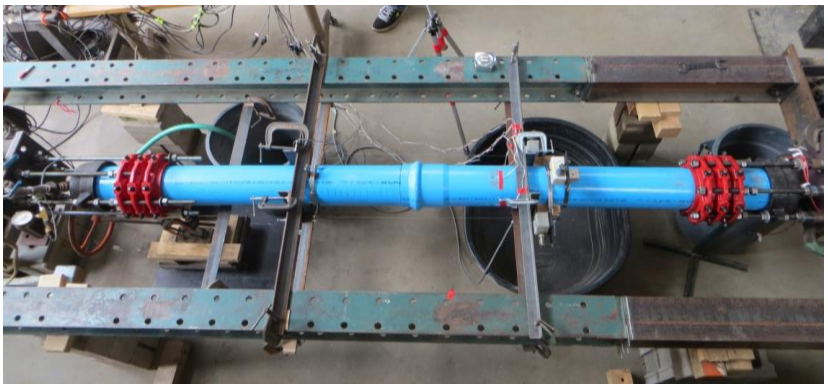

Figure 3.1. Test Setup for Test C1 (North is on the Right)

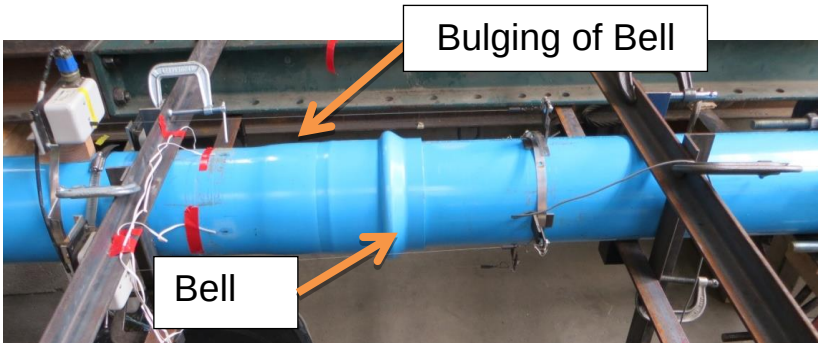

Figure 3.2. End of Test Condition for Test C1 (North is on the Left)

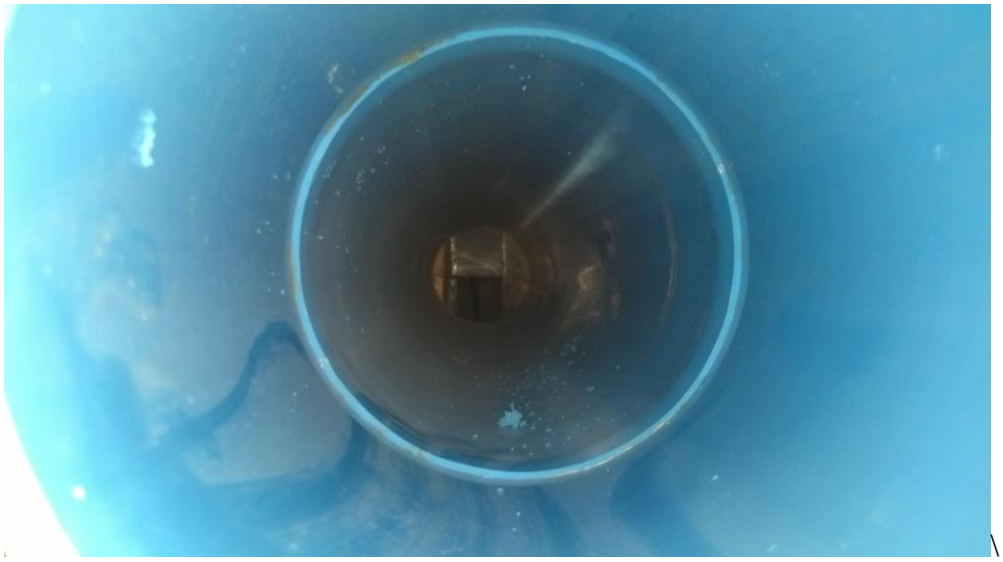

Figure 3.3. View of Interior of C1 Showing Pipe Spigot Pushed through Bell

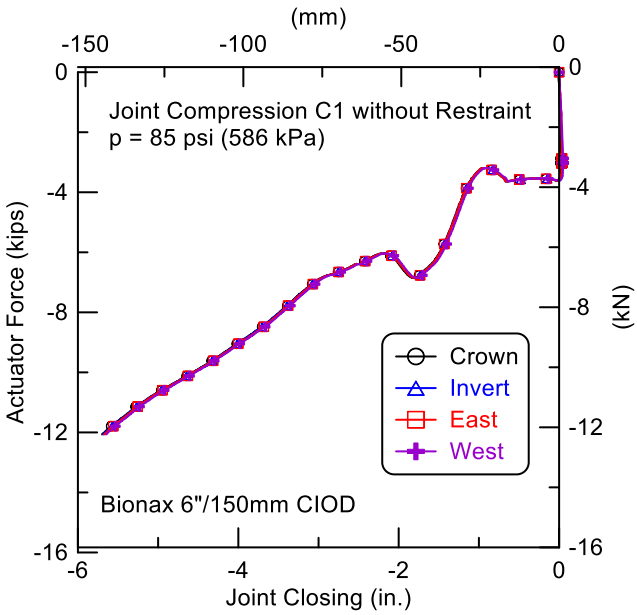

Figure 3.4. Joint Compression C1 – Force vs. Joint Closing

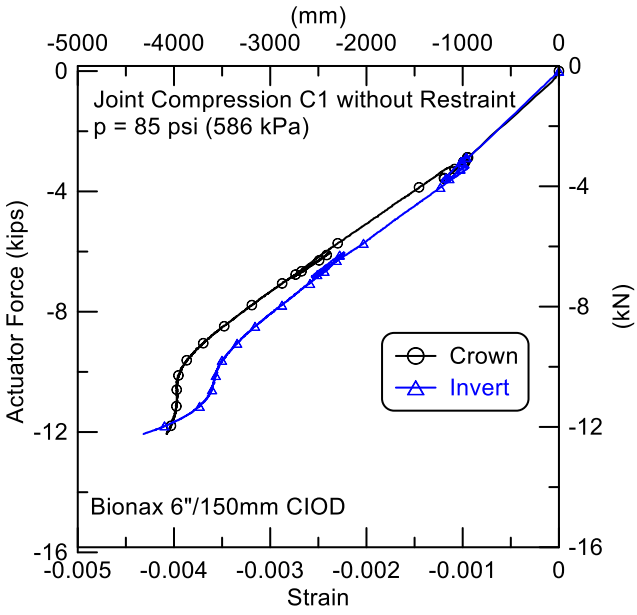

Figure 3.5. Joint Compression C1 – Axial Strain vs. Joint Closing

3.2 With Joint Restraint

Compression test C2 was a joint with a UFR1559-C-6-I restraint. The pipe section again was pressurized to approximately 85 psi (587 kPa).

Figure 3.6 is a photo of the test setup for test C2. In the photograph, north is to the right. String potentiometers were positioned at the crown, invert, east springline and west springline. Strain gages mounted in both the axial and hoop (circumferential) direction were mounted at the crown, invert, east springline, and west springline roughly 18 in. (457 mm) north of the joint. The maximum compressive force applied in test C2 was -19.4 kips (-86.7 kN), when the test was stopped at a displacement of -5.8 in. (-147.3 mm). Figure 3.7 shows a view of the interior of test C2 where the spigot end was simply pushing through the bell and bell restraint.

The compressive force vs. joint closing plots for the four string pots used in test C2 are shown in Figure 3.8. All string pot measurements were virtually identical. The axial strains at the crown and east and west springlines vs. actuator force are shown in Figure 3.9. Again, all strain gages were in good agreement. The axial strain gage at the invert was not functioning. Hoop strains for C2 vs. actuator force are shown in Figure 3.10. There appears to be an offset or gage seating effect for all gages at small strains. However, all readings show good agreement. Figure 3.11 shows average hoop vs. axial strain for C2. The seating at the early strains has been removed. The slope of the strain gage data shows an apparent Poisson ratio of $\nu = 0.41$.

3.3 Compression Test Comparison

Figure 3.12 compares the compressive push force vs. joint closure for tests C1 and C2. The addition of the restraint increased the compressive force required to push the spigot into the bell side of the pipe. Even with the restraint in place, the spigot was sufficiently ductile to reduce in size by circumferential wrinkling (see Fig. 3.7), and penetrate beyond the end of the bell through the circular clamp of the restraint. The specimen did not fail or rupture during either joint compression test. The spigot simply pushed through the unrestrained bell in test C1 and through the bell and restraint in test C2.

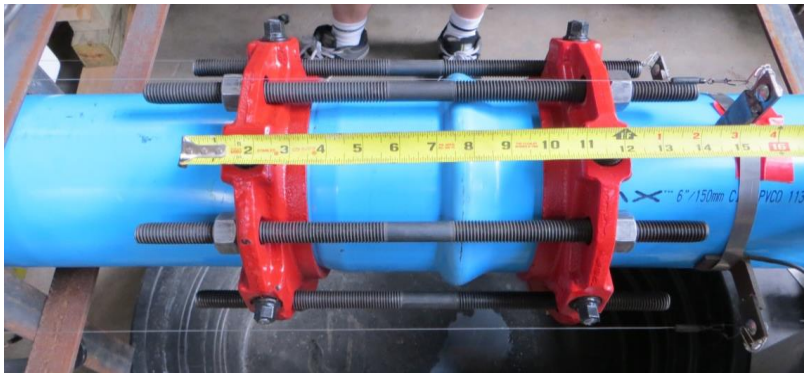

Figure 3.6. Test Setup for Test C2 (North is on the Right)

Figure 3.7. View of Interior of C2 Showing Pipe Spigot Pushing through Bell

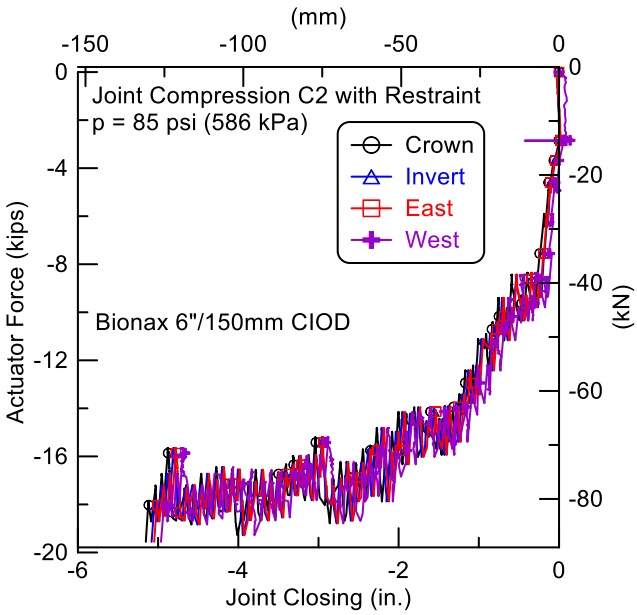

Figure 3.8. Joint Compression C2 – Force vs. Joint Opening

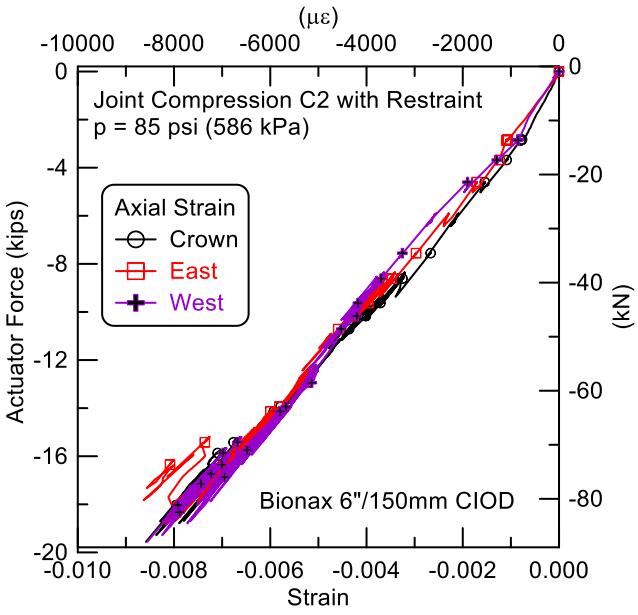

Figure 3.9. Joint Compression C2 – Axial Strain vs. Joint Opening

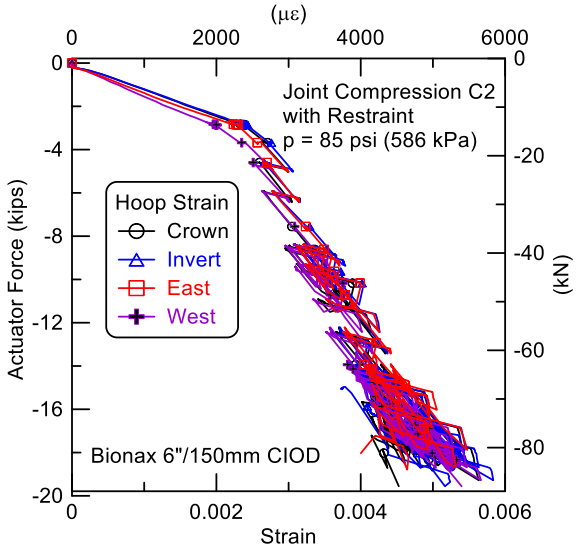

Figure 3.10. Joint Compression C2 – Force vs. Hoop Strain

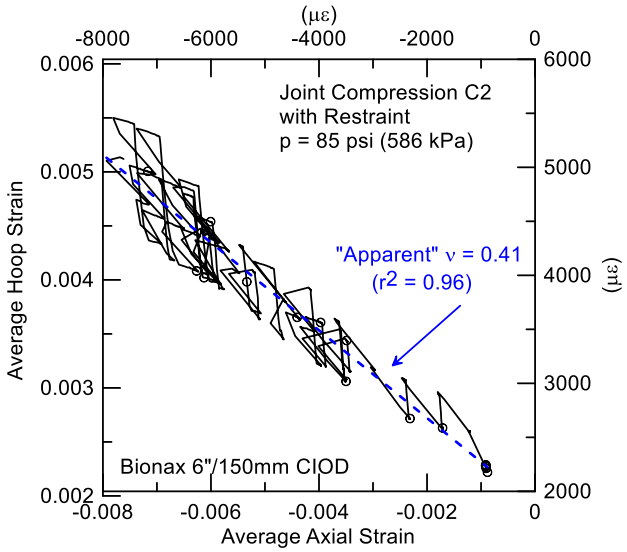

Figure 3.11. Joint Compression C2 – Hoop Strain vs. Axial Strain

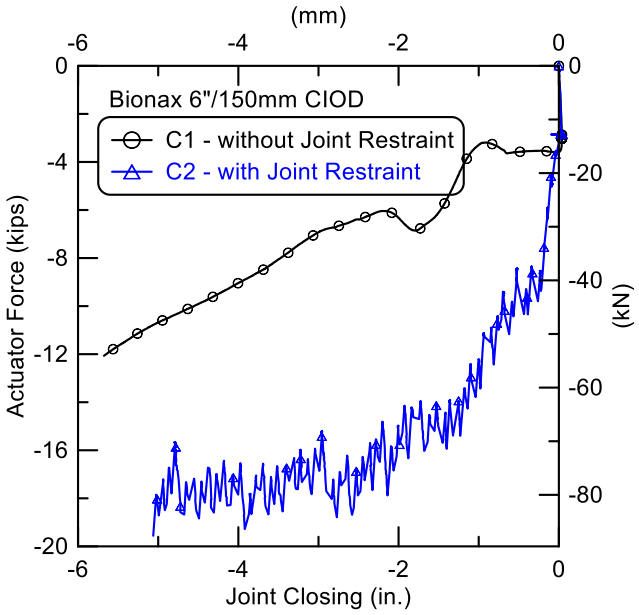

Figure 3.12. Joint Compression Tests C1 and C2 – Force vs. Joint Closing

4. Joint Tension Tests

4.1 Without Joint Restraint

Sections of Bionax were tested in tension without a joint restraint in test T1 and with a joint restraint in test T2. The pipes were fitted with end caps and pressurized to approximately 85 psi (587 kPa). During pressurization thrust forces were generated at the specimen end caps, which were resisted by clamps being held in a stationary position during this phase of loading. The initial load cell measurements reflect the restraining force needed to resist joint pullout under internal pressure.

String potentiometers were positioned at the crown, invert, east springline and west springline. Strain gages were mounted at the crown and invert roughly 30 in. (762 mm) south of the joint.

Figure 4.1 shows the end force developed as the pipe was pressurized. During pressurization the pipe was restrained in the longitudinal direction, so the internal pressure caused the pipe to contract in the axial direction. The contraction was caused by the Poisson's effect of negative strains that develop as positive circumferential strains are generated by internal pressure.

Figure 4.2 shows the east and west springline joint openings as the pipe was subjected to longitudinal tension. The pipe did not fail, and the test was stopped prior to joint pullout. The maximum force applied in test T1 was roughly -3.0 kips (-13.4 kN), which was generated to resist the thrust forces caused by internal pressure at the end caps of the pipe specimen. As the pipe specimen was pulled in extension, an average compressive load reduction of 200 lb (0.88 kN) was recorded. This reduction in restraining load is equal to the tensile pullout force generated as the spigot was pulled from the bell. Rather than measuring a direct pullout force, this test measured a reduction in resisting force, which is equivalent to the pullout force developed at the joint. The test was stopped at a displacement of 3.8 in. (96.5 mm).

Figures 4.3 and 4.4 show the axial strains and hoops strain, respectively, developed during tension test T1. The axial strain from the east and west gages were in excellent agreement, as were the east and west hoop strains. Figure 4.5 shows the axial vs. hoop strains during the tension test.

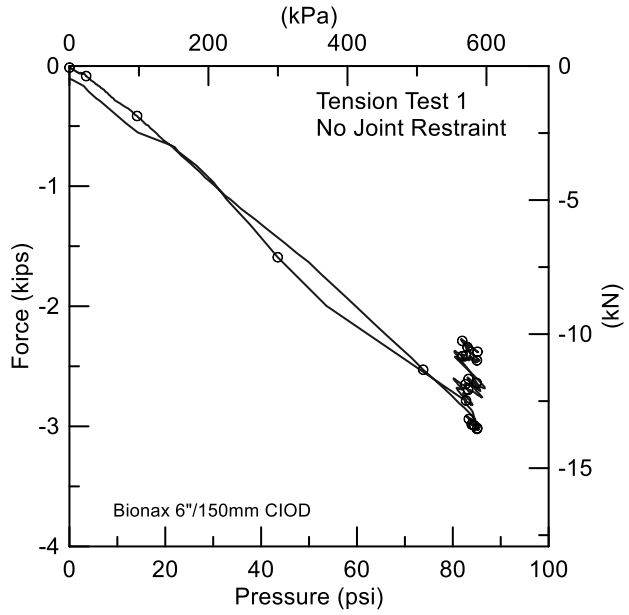

Figure 4.1. Joint Tension T1 – Force vs. Pressure

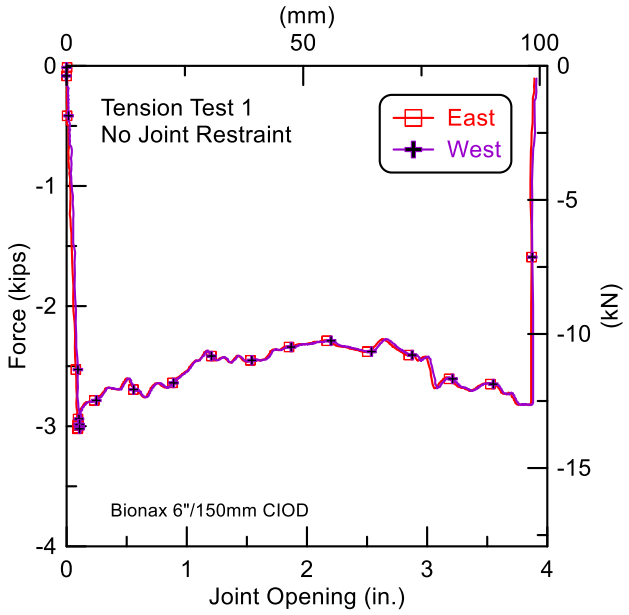

Figure 4.2. Joint Tension T1 – Force vs. Joint Opening

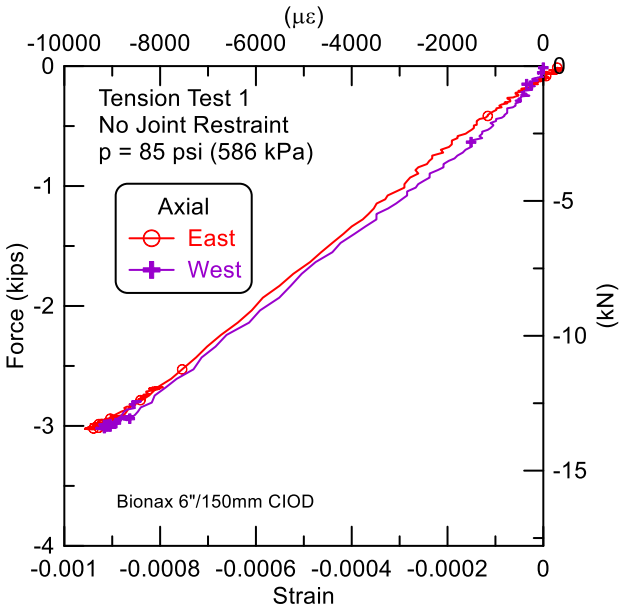

Figure 4.3. Joint Tension T1 – Force vs. Axial Strains

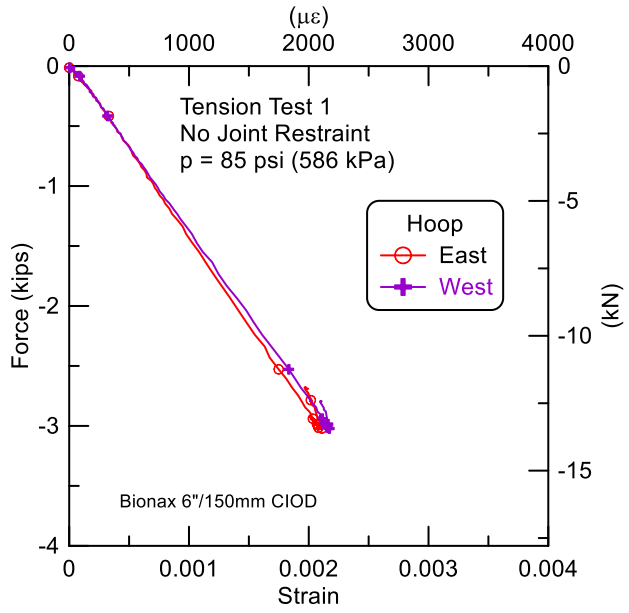

Figure 4.4. Joint Tension T1 – Force vs. Hoop Strains

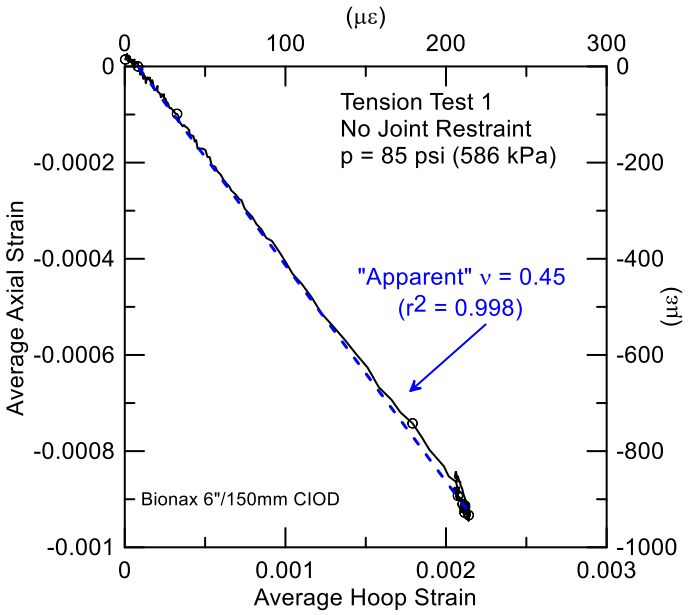

Figure 4.5. Joint Tension T1 – Hoop Strain vs. Axial Strain

4.2 With Joint Restraint

Sections of Bionax were tested in tension with a joint restraint. The pipes were fitted with end caps and pressurized to approximately 85 psi (586 kPa).

Figure 4.6 is a drawing of the basic setup for tension test T2, showing the position of the joint restraints, string pots, and strain gage planes. String potentiometers were positioned around the joint restraint to measure joint and relative restraint movements. Strain gages were mounted 24.5 in. (622.3 mm) north and 21 in. (533.4 mm) south of the bell. Figures 4.7 and 4.8 are photos of the setup for test T2.

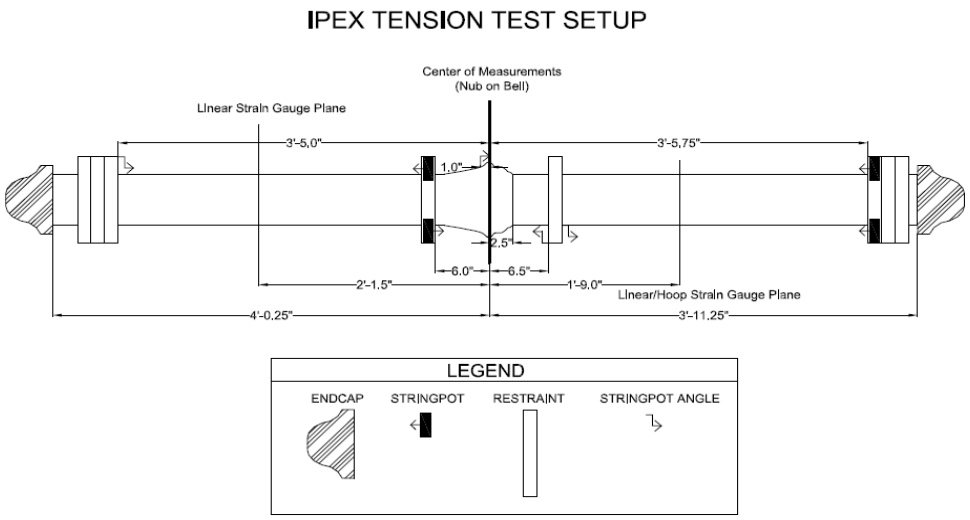

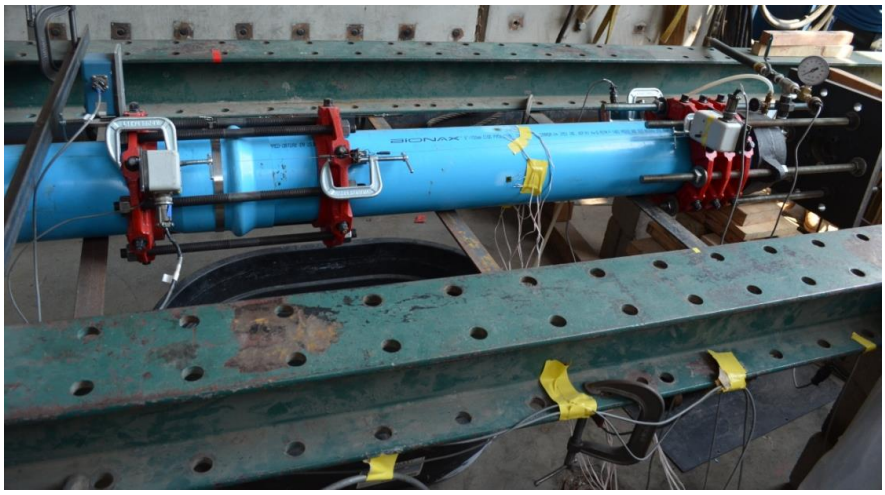

Figure 4.7. Tension Test T2 Prior to Test (North is to the Left)

Figure 4.8. Close-Up View of T2 Prior to Test (North is to the Right)

Figures 4.9 and 4.10 show the axial and hoop strains, respectively, developed in the pipe section during pressurization. Even though the section was "fixed" at the north and south ends, a small amount of axial strains developed during pressurization. As positive tensile strains were generated by internal pressure, negative compressive strains were induced by the Poisson's effect. These strains were resisted by the clamping force mobilized by the restraint, resulting in axial contraction that was markedly less than that associated with test T1. The hoop strains are much larger as the pipe expanded circumferentially during pressurization.

Figure 4.11 shows the axial strains at four locations around bell of the specimen as tension was applied. All axial strains are tensile. The strains in the hoop direction on the spigot side are shown in Figure 4.12. Since the pipe was pressurized, the hoop strains initially were positive. As the specimen was pulled, the tensile hoop strains became negative due to the Poisson effect as the specimen elongated.

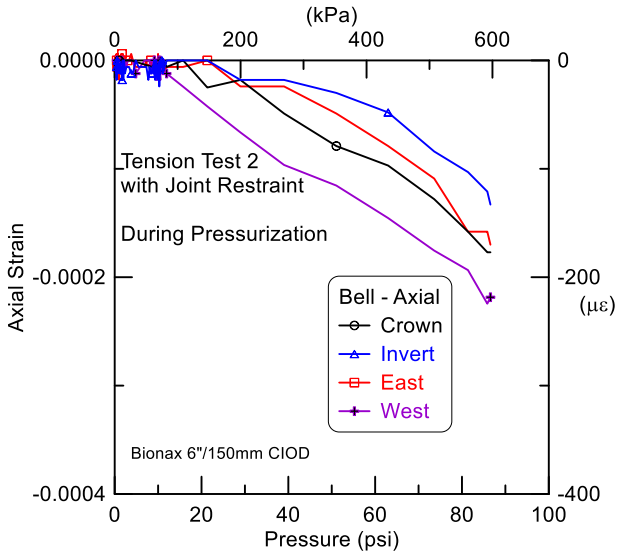

Figure 4.9. Joint Tension T2 – Bell Side Axial Strains during Pressurization

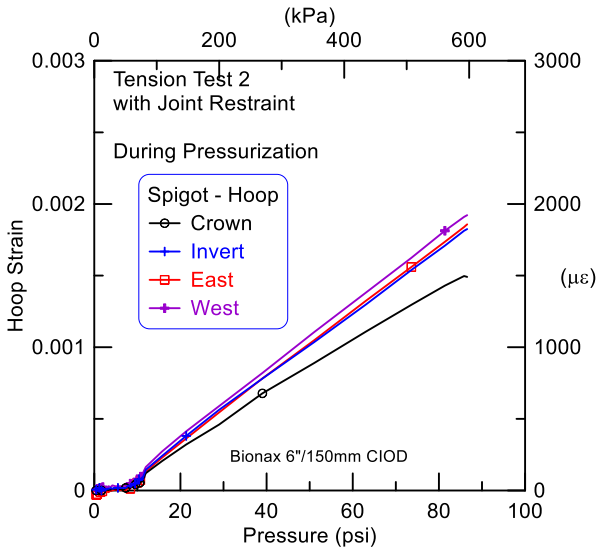

Figure 4.10. Joint Tension T2 – Spigot Side Hoop Strains during Pressurization

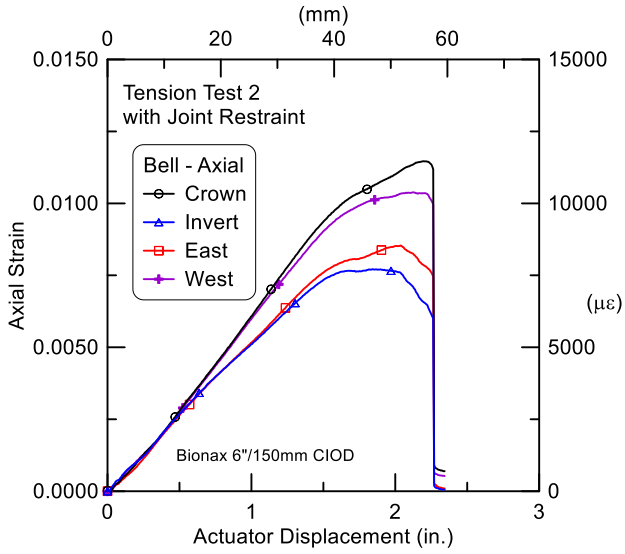

Figure 4.11. Joint Tension T2 – Axial Strain vs. Actuator Displacement

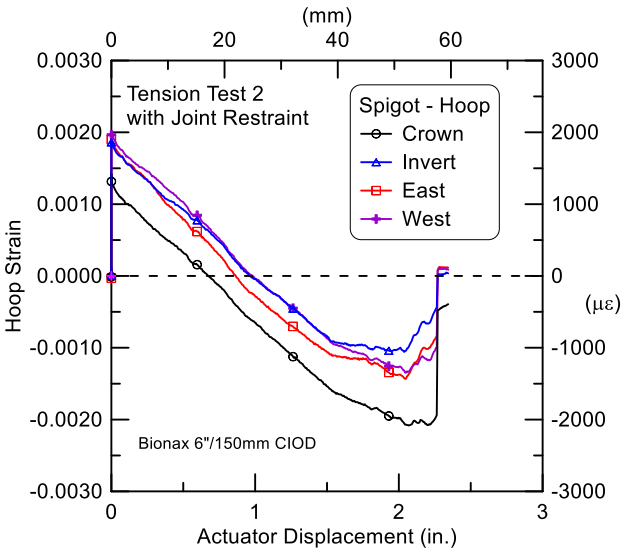

Figure 4.12. Joint Tension T2 – Force vs. Hoop Strains

Figure 4.13 shows the average strains vs. actuator displacement for test T2. In the figure, the axial strains increase as the tension test proceeds, reaching an average axial strain level of approximately 0.8% when joint failure occurred. The hoop strains start positive, due to the existing strains from pressurization. As the specimen was strained longitudinally the hoops strains became compressive due to the Poisson effect.

Figure 4.14 shows the tension force-actuator displacement test results for test T2. The peak applied force was 17.9 kips (79.4 kN) at a displacement of 2.04 in. (51.8 mm). The pipe ruptured near the bell side joint restraint at a force of 16.1 kips (71.5 kN) at a failure actuator displacement of 2.26 in. (51.8 mm). Figure 4.15 is a photograph of water leaking under pressure at the time of rupture. Figure 4.16 is a closer view of the ruptured pipe.

The joint restraint slipped slightly on the spigot side of the joint, after which the metal clamps of the collar penetrated the underside of the pipe, causing a stress concentration. As the test continued the pipe could no longer accommodate the additional strains that were concentrated at the joint restraint, and the pipe ruptured.

Figures 4.17 and 4.18 show measurements from the four string potentiometers used for T2. The "North (1)" pot was connected from the north fixed end to the north joint restraint (bell side). The "Center (2)" pot measured the movements between the north (bell side) and south (spigot side) restraint collars. The "South – West (3)" pot was connected from the south fixed end to the restraint on the spigot side of the joint. The "South – East to Bell (4)" pot was connected from the south fixed end to a location just past the bell.

The "North (1)" pot measurements show that the bell side (north section) was continuously straining as the tension force was applied. The "Center (2)" pot measurements show zero movement between the joint restraint collars. The "South – West (3) measurement showed the spigot side (south section) was continuously straining during the test. The sum of the (1), (2), and (3) measurements is compared with the applied actuator force in Figure 4.16. The final sum of the three pots is 2.22 in. (56.4 mm). The actuator displacement at pipe rupture was 2.26 in. (57.54 mm), in close agreement with the string pot summation.

The difference between string pot (4) and pot (3) represents the joint opening of T2. The difference at pipe rupture was 0.41 in. (10.4 mm).

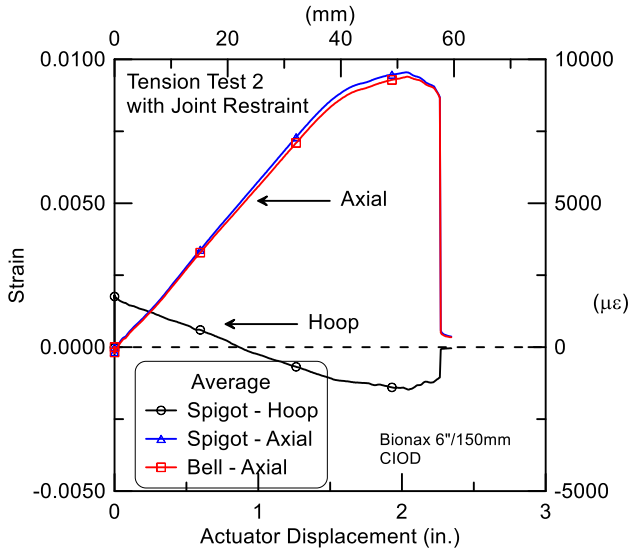

Figure 4.13. Joint Tension T2 – Average Axial an Hoop Strains vs. Actuator Displacement

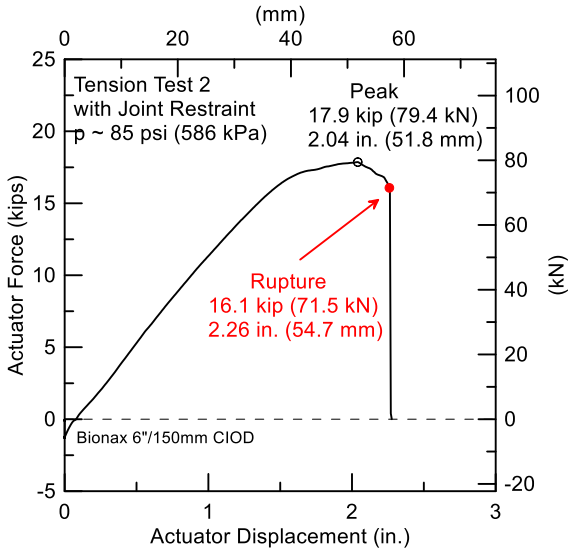

Figure 4.14. Joint Tension T2 – Actuator Force vs. Actuator Displacement

Figure 4.15. Joint Tension T2 – Pipe Rupture

Figure 4.16. Joint Tension T2 – Close Up of Ruptured Pipe

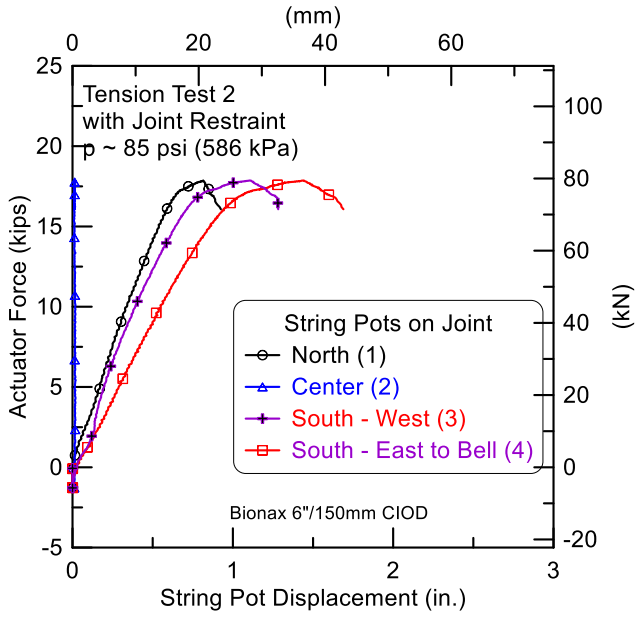

Figure 4.17. Joint Tension T2 - String Pots vs. Actuator Force

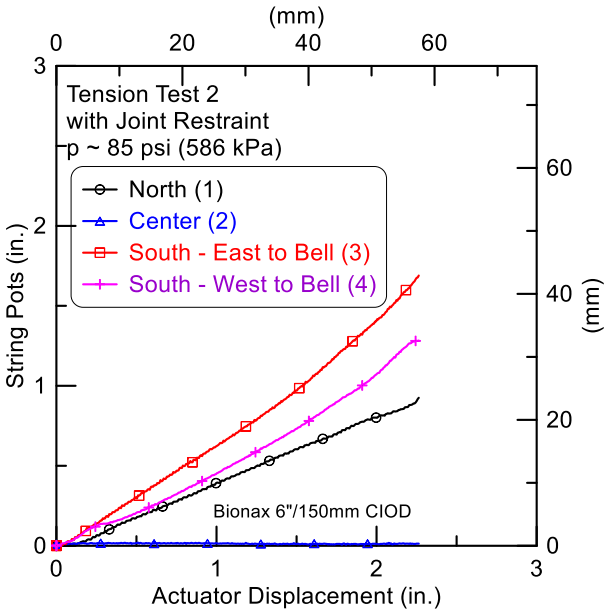

Figure 4.18. Joint Tension T2 - String Pots vs. Actuator Displacement

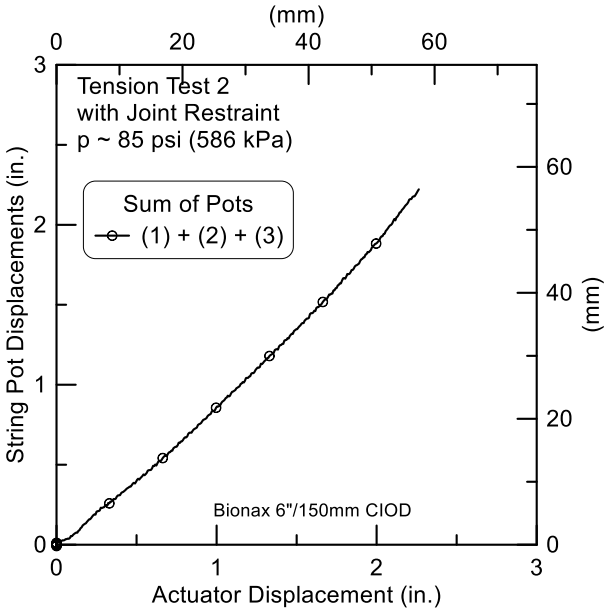

Figure 4.19. Joint Tension T2 – Sum of String Pots vs. Actuator Displacement

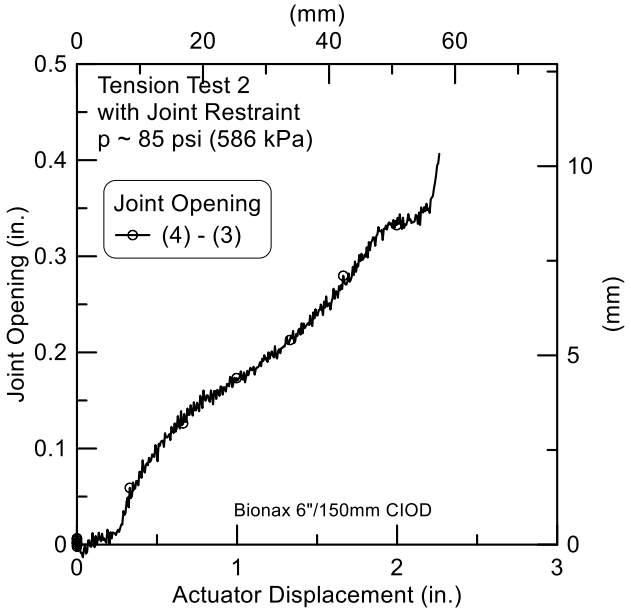

Figure 4.20. Joint Tension T2 – Joint Opening vs. Actuator Displacement

5. Summary

Tests were performed to characterize Bionax stress-strain-strength characteristics and the strength of joints in tension and compression. Eleven tensile test coupons were tested at various strain rates to evaluate the strength of the Bionax and Young's Modulus at relatively small strains. Table 5.1 summarizes the tensile coupon test data.

Tension and compression tests with and without joint restraints were performed on Bionax pipes. The pipes were pressurized to an internal water pressure of 85 psi (586 kPa). In the compression tests, pipe failure did not occur. The spigot end was pushed into the bell. The restrained pipe joint tension test experienced rupture at the bell side of the restraint. The joint and restraint slipped a small amount and the clamp regripped. Additional tension caused a rupture of the pipe wall. Table 5.2 summarizes the joint compression and tension test results.

Figure 5.1 compares the joint capacity in compression (C2) and tension (T2) with a joint restraint. In test C2 the spigot end pushed through the bell and continued to be pushed beyond the exterior restraint. Test T2 was the only test where the pipe ruptured. The rupture occurred near a restraint, initiating from a stress concentration where the restraining clamp gripped the pipe.

Table 5.1. Bionax Tensile Coupon Data

	Young's Modulus ksi (GPa)	Poisson's Ratio	Maximum Stress ksi (MPa)	Strain at Maximum Stress
Average	433 (2.99)	0.36	8.34 (57.5)	0.0507
Stdev	53.7 (0.44)	-	0.39 (2.7)	0.0028

Table 5.2. Bionax Joint Compression and Tension Test Data

Specimen	Joint Condition	Maximum Force kips (kN)	Joint Opening at Maximum Force in. (mm)
Compression C1	No Restraint	-12.1 (-54.2)	-5.7 (-144.8)
Compression C2	Restraint	-19.4 (-86.7)	-5.8 (-147.3)
Tension T1	No Restraint	0.2 (0.88)[1]	3.8 (96.5)
Tension T2	Restraint	17.9 (79.4)	2.3 (51.8)

1- tensile pullout force equal to reduction in initial compressive force that was mobilized to resist thrust from internal pressure on the specimen end caps.

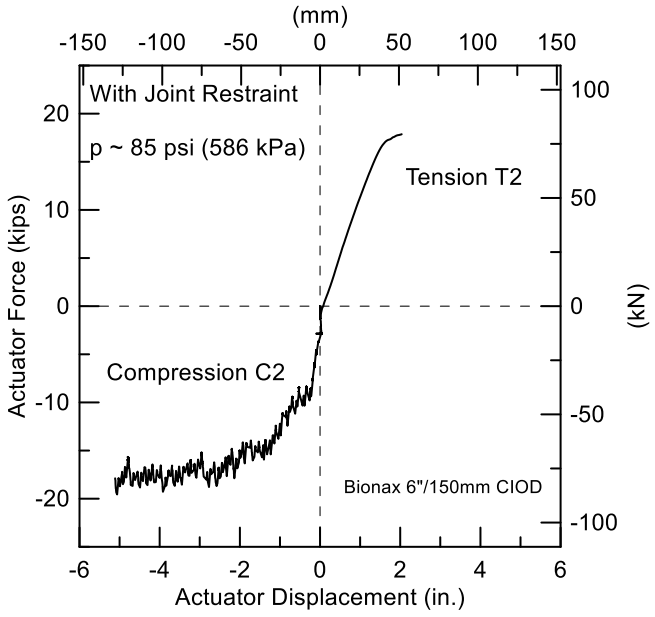

Figure 5.1. Joint Compression and Tension Tests (C2 and T2) with Joint Restraint